SCIENCE CHINA
Information Sciences

• RESEARCH PAPER •

September 2025, Vol. 68, Iss. 9, 192207:1–192207:18
https://doi.org/10.1007/s11432-024-4336-y

Adaptive tracking control of uncertain strict-feedback systems with tight self-adjustable performance guarantees

Hai-Xiu XIE, Jin-Xi ZHANG* & Tianyou CHAI

State Key Laboratory of Synthetical Automation for Process Industries, Northeastern University, Shenyang 110819, China

Received 5 March 2024/Revised 9 October 2024/Accepted 12 March 2025/Published online 30 July 2025

Abstract This paper is concerned with the problem of fast accurate reference tracking for the strict-feedback systems with parametric uncertainties and unmatched disturbances. It is focused on the case where the transient response of the tracking error, except for the settling time, e.g., the overshoot, is taken into consideration in the context of ensuring the natural satisfaction of the initial condition. This significantly challenges the existing high-performance control solutions which are developed by means of the tuning function-based initialization technique, the performance funnel with an infinitely large entry, or the exponential function related to the initial tracking error. To conquer this obstruction, a novel adaptive prescribed performance control strategy is put forward in this paper. Herein, an error transformation based on a reverse tuning function is skillfully combined with the constraint-handling method to form a tight performance envelope on the tracking error. In addition, a set of self-adjustable, asymmetric and time-varying performance functions are further constructed to enhance the reliability of control designs. It turns out that the user-specified transient and steady-state tracking performance and the boundedness of all the signals in the control system are guaranteed by our approach. The above theoretical findings are substantiated via three simulation studies.

Keywords adaptive control, model uncertainties, prescribed performance, reference tracking, strict-feedback systems

Citation Xie H-X, Zhang J-X, Chai T Y. Adaptive tracking control of uncertain strict-feedback systems with tight self-adjustable performance guarantees. Sci China Inf Sci, 2025, 68(9): 192207, https://doi.org/10.1007/s11432-024-4336-y

1 Introduction

Recent decades have witnessed an intense level of research activity on tracking control of uncertain strict-feedback nonlinear systems [1–5]. This is motivated by their theoretical interests and practical significance. On the one hand, the presence of uncertainties renders the controller design of such systems a challenging task. If not handled well, they will result in performance degradation and even instability of the control system. On the other hand, plenty of physical plants can be described by or transformed to the strict-feedback form, such as the robotic manipulator [4], the jet engine compressor [6], and the ship autopilot [7].

Fast accurate reference tracking is frequently desirable in practical applications, which is conducive to ensuring the safety and reliability of system operation. In this direction, a variety of high-performance control approaches were developed, primarily based on funnel control (FC) [8–12] and prescribed performance control (PPC) [13–17]. They allow the designer to quantitatively predefine the transient and steady-state behavior of the tracking error. Up to now, both of them have been skillfully combined with adaptive control [18, 19] and fuzzy/neural network control [20, 21] to improve the tracking performance of parametrically uncertain and unknown nonlinear systems, respectively. It is noteworthy that the results [11–21] necessitate a requirement for the feasible initial condition in the sense that the initial value of the constrained error should be within the performance envelope. This means that when the system is rerun, or the reference is changed, these results need to check whether or not the initial condition is met. If it is not met, the performance function needs to be reselected according to the initial condition of the closed-loop system. This process complicates the design and implementation of the controller. Intuitively, the employment of the performance function with a large initial value [19] contributes to alleviating the

* Corresponding author (email: zhangjx@mail.neu.edu.cn)

problem mentioned above. However, this is a palliative, not a cure, because the verification of the initial condition is still necessary in the event of a relatively large initial error. Furthermore, the performance envelope with an enlarged entry may render the overshoot regulation of the tracking error infeasible.

Currently, there are three mainstream methods to ensure the natural satisfaction of the initial condition. The first one is adopting the tuning function [22, 23] to adjust the tracking error and then imposing the performance constraint on the adjusted error. By this means, it is achieved that the tracking error enters into the preselected performance envelope within the preassigned settling time. Unfortunately, the explicit performance boundary during the transient phase fails to be predefined, thus lacking a consideration of the transient response of the tracking error except for the settling time, e.g., the overshoot. The second one is constructing a performance function with an infinitely large initial value [24–27] such that the initial condition holds naturally. To accelerate error convergence, the predefined settling time was further realized [28, 29]. Thereafter, the extension to the asymmetric performance constraint [30–32] was successfully performed, which achieves reference tracking with the user-specified overshoot, settling time and accuracy under the known sign of the initial tracking error. Nevertheless, the tracking error is constrained by the asymmetric performance funnel with an infinitely large entry. This may lead to a poor transient behavior, e.g., a large positive (negative) error peak in the case of the positive (negative) initial error. The third one is forming a performance function whose initial value is related to the initial tracking error, thereby automatically matching arbitrary known initial conditions [33–39]. In this way, the full-time performance constraint is imposed on the tracking error, effectively avoiding the oversized error overshoot and peak. Even so, it should be noted that the settling time is determined collectively by two adjustable parameters [34–36], complicating the formulation of performance specifications, and just the exponential convergence is achieved [37]. Besides, the second-order and higher-order derivatives of the reference are necessary [22, 25, 26, 28, 30, 32, 34–37, 39]; the virtual control coefficients are required to be constant [23, 25, 26, 29, 34, 35, 37] or known [31, 34, 35, 37]; the disturbances are ignored [26, 34–36, 39] or should be differentiable [37]. On the other hand, tedious derivative calculations of the virtual control signals have to be made in the controller design [22, 25, 26, 28, 29, 32, 34, 35, 37, 39], leading to the problem of "explosion of complexity".

It is also notable that the existing high-performance control results [8, 9, 11, 13–29, 32–34, 36–39] commonly choose a pair of monotonically time-varying functions to form an inelastic performance funnel imposed on the tracking error for ease of predefining the requisite transient and steady-state response. In some practical applications, nevertheless, the paroxysmal factors, e.g., a disturbance with a large amplitude of change or a highly fluctuating reference, may increase the tracking error, rendering it much closer to the performance boundary. This likely gives rise to constraint violation in the case of low-frequency sampling of the computer control system, especially when the performance specifications are too strict. Therefore, widening the performance boundary in a proactive manner is sometimes beneficial for control implementation in the presence of some paroxysmal factors, despite the relaxation of the performance specifications, as pointed out by [10, 30]. A typical example is performance-related constrained control of unmanned aerial vehicles in the adverse airflow condition [40], wherein the flight controller needs to make a trade-off between the control performance and the vehicle capability for a safe and stable flight. Until now, some pioneering studies have been conducted for various scenarios, including the input saturation [41–44], the strong external disturbances [31, 40, 45], the drastically changed reference [46], and the quasi-periodic denial-of-service attack [47]. Nonetheless, these solutions are established in the cases of the known virtual control coefficients [31, 40–42, 47], the state-dependent [40] or differentiable [41, 42] disturbances, the completely known additive nonlinearities [40–42], or the feasible initial condition [40–47].

The above observations indicate that on the premise of ensuring the natural satisfaction of the initial condition, the high-performance tracking control problem for strict-feedback systems with parametric uncertainties and unmatched disturbances remains open. It further becomes challenging under the cases where neither the values of the state-dependent virtual control coefficients nor their bounds are known; the disturbances are not necessarily differentiable or state-dependent; the second-order and higher-order derivatives of the reference do not need to be available; tedious derivative calculations of the virtual control signals do not have to be made in the recursive design. In this paper, a robust adaptive PPC approach is developed. Its superiority is enumerated as follows.

- Although the problem of the initial condition in the classical PPC methods [11–21, 40–47] is addressed in the existing studies on high-performance control [22–32, 37], the transient tracking performance fails to be quantitatively determined, e.g., the overshoot regulation of the tracking error. Therefore, an error transformation based on a reverse tuning function is skillfully combined with the constraint-handling

method. The resulting control achieves reference tracking with the predefined overshoot, settling time and accuracy, while ensuring the natural satisfaction of the initial condition.

• Contrary to the performance functions in the preassigned fixed forms [8–11, 13–30, 32–34, 36–39], a pair of self-adjustable performance functions are constructed. This evades violation of the performance constraint induced by the paroxysmal factors, e.g., disturbances with large amplitude of change, in the case of low-frequency sampling of a control system. On the other hand, the differentiability of the performance functions is guaranteed. This avoids the potential non-differentiable problem of the self-adjustable performance functions [45] due to the absolute value of the error derivative, which is incompatible with the dynamic surface control technique.

The rest of the paper is organized as follows. Section 2 formulates the problem under consideration. Section 3 presents the controller development and conducts the performance analysis to validate its effectiveness, which is extended to the self-adjustable performance constraint in Section 4. In Section 5, the theoretical findings are illustrated by three simulation studies. In the end, Section 6 concludes this paper.

2 Problem formulation and preliminaries

2.1 System description

The strict-feedback systems under consideration are described by

$$\begin{cases} \dot{x}_i = f_i(\overline{x}_i) + g_i(\overline{x}_i)x_{i+1} + d_i(t), \quad i = 1, \ldots, n-1, \\ \dot{x}_n = f_n(\overline{x}_n) + g_n(\overline{x}_n)u + d_n(t), \\ y = x_1, \end{cases} \tag{1}$$

where $\overline{x}_i = [x_1, \ldots, x_i]^{\mathrm{T}} \in \mathbb{R}^i$, $i = 1, \ldots, n$; $\overline{x}_n$ and $y \in \mathbb{R}$ denote the system state and the system output, respectively; $f_i(\overline{x}_i) \in \mathbb{R}$ and $g_i(\overline{x}_i) \in \mathbb{R}$, $i = 1, \ldots, n$, are the nonlinear functions; $d_i(t) \in \mathbb{R}$, $i = 1, \ldots, n$, represent the external disturbances; $u \in \mathbb{R}$ stands for the control input.

Three widely used assumptions for (1) are made as follows.

Assumption 1 (see [28]). There exist an unknown constant, $\delta_i \geqslant 0$, and a known continuously differentiable function, $\Psi_i(\overline{x}_i) \geqslant 0$, such that

$$|f_i(\overline{x}_i)| \leqslant \delta_i \Psi_i(\overline{x}_i), \quad i = 1, \ldots, n. \tag{2}$$

Assumption 2 (see [15, 22, 32]). The function, $g_i(\overline{x}_i)$, is unknown and continuously differentiable with respect to $\overline{x}_i$, $i = 1, \ldots, n$. Moreover, there exist unknown constants, $\underline{g}_i > 0$ and $\overline{g}_i > 0$, such that $\underline{g}_i \leqslant |g_i(\overline{x}_i)| \leqslant \overline{g}_i$, $i = 1, \ldots, n$. Without loss of generality, let $\underline{g}_i \leqslant g_i(\overline{x}_i) \leqslant \overline{g}_i$, $i = 1, \ldots, n$.

Assumption 3 (see [28, 43]). The disturbances are unknown, piecewise continuous in time, and uniformly bounded, i.e., $|d_i(t)| < \overline{d}_i$ for all $t \geqslant 0$ with $\overline{d}_i$ being an unknown positive constant, $i = 1, \ldots, n$.

2.2 Control objective

The control goal for (1) is fast accurate reference tracking, i.e., steer its output, $y(t)$, to track a reference, $y_r(t)$, with satisfactory performance, where the tracking error is denoted by $e(t) = y(t) - y_r(t)$. Specifically, the requisite transient and steady-state tracking behavior is prescribed by

$$-\rho_l < e(t) < \rho_u, \quad t \geqslant T_f, \tag{3}$$

where the accuracy, ρ_l and ρ_u, and the settling time, T_f, are positive constants.

A common assumption and a pair of technical lemmas are introduced below.

Assumption 4 (see [1, 2, 18]). The reference, $y_r(t)$, and its first-order time derivative, $\dot{y}_r(t)$, are uniformly bounded and available. In addition, the second-order time derivative, $\ddot{y}_r(t)$, is uniformly bounded yet unknown.

Lemma 1 (see [18]). For any $\sigma > 0$ and $\varrho \in \mathbb{R}$, there holds $0 \leqslant |\varrho| - \frac{2}{\pi}\varrho \arctan\left(\frac{\varrho}{\sigma}\right) < \frac{2}{\pi}\sigma$.

Lemma 2 (see [48]). Consider the dynamic system $\dot{\varpi}(t) = -\gamma_1\varpi(t)+\gamma_2\beta(t)$ with the constants $\gamma_1 > 0$ as well as $\gamma_2 > 0$ and the function $\beta(t) \geqslant 0$. For a given initial condition $0 \leqslant \varpi(t_0) < \infty$, there holds $\varpi(t) \geqslant 0$, $\forall t \geqslant t_0$. If additionally $0 \leqslant \beta(t) < \infty$, $\forall t \geqslant t_0$, then one has $0 \leqslant \varpi(t) < \infty$, $\forall t \geqslant t_0$.

Remark 1. Assumption 1 is widely adopted in the existing studies on control of strict-feedback systems [22,28,30,32,39]. Therein, $\Psi_i(\overline{x}_i)$, $i = 1, \ldots, n$, are known as the core functions and can be easily extracted only based on the deep-rooted information of the plant. This renders the additive nonlinearities of (1) less restrictive and more general than the ones directly characterized by linearly parameterized functions [3,4, 18,19,26,31,35]. Additionally, the requirement for the core functions being smooth [22,32,39] is removed. As for Assumption 2, the presence of $\underline{g}_i$, $i = 1, \ldots, n$, aims to ensure the controllability of (1); otherwise, Eq. (1) becomes uncontrollable when $g_i(\overline{x}_i)$ tends to or equals to zero, $i \in \{1, \ldots, n\}$. Assumption 3 is commonly used and reasonable in the literature. On the one hand, the disturbances are bounded in the real world. On the other hand, Assumption 3 implies that the disturbances meet the local Lipschitz condition without the assumptions on the differentiable [37, 41, 42] or state-dependent [40] disturbances. This, together with Assumptions 1 and 2, guarantees the existence and uniqueness of the solution of (1) [15]. In the classical studies on backstepping control designs [20, 22, 25, 26, 28, 30, 32, 34–37, 39], $y_r(t)$ is required to be differentiable up to the relative degree of the plant, and these derivatives should be available for controller implementation. In this paper, such a requirement is relaxed to Assumption 4 with the help of the dynamic surface control technique [1, 2, 18, 19, 40–42].

To sum up, the problem studied in this paper reads as follows.

Problem 1. For the strict-feedback system in (1) with parametric uncertainties and unmatched disturbances, design a controller such that the behavior of the tracking error can be prescribed on $[0, T_f)$ under any known initial condition; the performance requirement in (3) is fulfilled; all the signals in the control system are bounded.

Remark 2. Notably, the problem of fast accurate reference tracking for the nonlinear systems has been extensively studied by the PPC method. Nevertheless, the majority of related results need to check whether or not the initial condition holds [11–21, 40–47], when the control system is rerun or the reference is changed. On the other hand, despite the natural satisfaction of the initial condition, there is no consideration of the transient response of the tracking error except for the settling time, e.g., the overshoot [22–32,37]. Either of the aspects mentioned above renders Problem 1 still open in the literature.

2.3 Reverse tuning function

For the sake of fulfilling practical prescribed-time reference tracking, a reverse tuning function, $\phi(t)$, is first used to adjust the tracking error, which satisfies (i) $\phi(t)$ is at least $\mathbb{C}^2$ with $\phi(0) = 1$, and (ii) $\lim_{t\to T_f} \phi(t) = 0$ and $\phi(t) = 0$ for $t \geqslant T_f$, where $T_f > 0$ is given in (3). For example, let

$$\phi(t) = \begin{cases} \sin^{\lambda+2}\left(\frac{\pi}{2T_f}(T_f - t)\right), & \text{if } 0 \leqslant t < T_f, \\ 0, & \text{otherwise,} \end{cases} \tag{4}$$

where λ is an adjustable positive constant determining the convergence speed of $\phi(t)$.

Remark 3. The function, $\psi(t)$, devised in [34, 35] can also be selected as a reverse tuning function (although it does not satisfy item (ii) enumerated above), i.e., $\psi(t) = \mathrm{e}^{-\zeta\omega_n t}(\cos(\omega_d t)+\frac{\zeta}{\sqrt{1-\zeta^2}}\sin(\omega_d t))$, where $0 < \zeta < 1$, ω_n, and $\omega_d = \omega_n\sqrt{1-\zeta^2}$ denote the damping ratio, the undamped natural frequency, and the damped natural frequency, respectively. In contrast with the settling time of $\psi(t)$ that is obtained by $t_s = 4/(\zeta\omega_n)$ under 2% criterion, the settling time of $\phi(t)$ can be given directly in advance due to the freedom of choosing T_f. Therefore, a more flexible selection of the reverse tuning function is provided in this paper.

Motivated by [34, 35], we employ (4) to adjust the tracking error and then get a new error variable, $\xi(t)$, with a zero initial value:

$$\xi(t) = e(t) - \phi(t)e(0). \tag{5}$$

In this way, the performance specification in (3) is formulated by

$$-\rho_l < \xi(t) < \rho_u, \quad \forall t \geqslant 0. \tag{6}$$

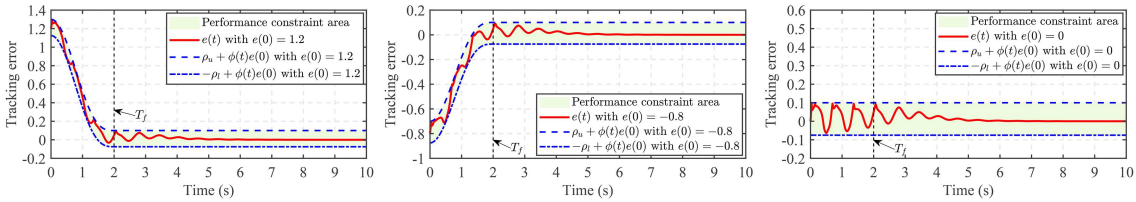

Figure 1 (Color online) Graphical representation of (6) with (5) in the cases of $e(0)=1.2>0$, $e(0)=-0.8<0$, and $e(0)=0$.

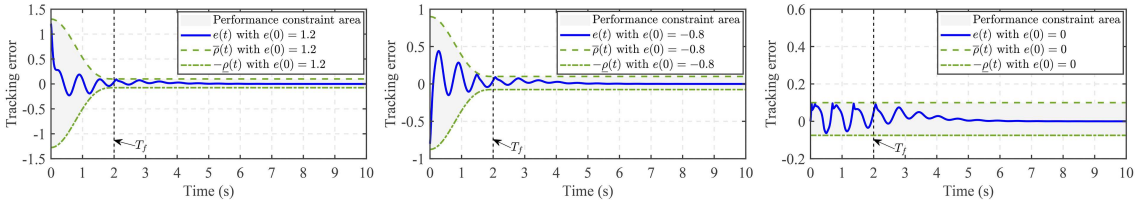

Figure 2 (Color online) Graphical representation of $-\underline{\rho}(t)<e(t)<\overline{\rho}(t)$ in the cases of $e(0)=1.2>0$, $e(0)=-0.8<0$, and $e(0)=0$.

Remark 4. Under any known $y(0)$ and $y_r(0)$, if Eq. (6) holds, then the following features are acquired.

- The initial condition is satisfied naturally, in the sense that $-\rho_l<\xi(0)<\rho_u \Leftrightarrow -\rho_l+e(0)<e(0)<\rho_u+e(0)$ with $\xi(0)=e(0)-\phi(0)e(0)=0$.
- The behavior of the tracking error can be prescribed over $[0,T_f)$, due to $-\rho_l+\phi(t)e(0)<e(t)<\rho_u+\phi(t)e(0)$, $t\in[0,T_f)$.
- From $\xi(t)=e(t)=y(t)-y_r(t)$, $t\geqslant T_f$, there holds $-\rho_l<e(t)<\rho_u$, $t\geqslant T_f$.
- The tight performance constraint on the tracking error is fulfilled for all $t\geqslant 0$. Compared with the state-of-the-art studies [22–32], the performance indices for the overshoot and settling time are regulated quantitatively. Besides, the performance envelope formed by $(-\rho_l+\phi(t)e(0))$ and $(\rho_u+\phi(t)e(0))$ is narrower than the performance envelope formulated by $-\underline{\rho}(t)$ and $\overline{\rho}(t)$ for all $t\geqslant 0$, where $\underline{\rho}(t)=\underline{\rho}_0\phi(t)+\rho_l$ and $\overline{\rho}(t)=\overline{\rho}_0\phi(t)+\rho_u$ with $\underline{\rho}_0=\overline{\rho}_0=|e(0)|$ are chosen by referring to [21,37]. The compared results are graphically illustrated in Figures 1 and 2.

2.4 Barrier function

For the purpose of (6), a barrier function, $\eta(t)=\eta(\xi(t))$, is adopted [43,49], which fulfills (i) $\eta(t)$ is at least $\mathbb{C}^2$ and strictly increasing for $\xi(t)\in(-\rho_l,\rho_u)$; (ii) $\lim_{\xi(t)\to(-\rho_l)^+}\eta(t)=-\infty$ and $\lim_{\xi(t)\to\rho_u^-}\eta(t)=+\infty$; (iii) $\eta(t)$ is bounded as $\xi(t)$ evolves inside $(-\rho_l,\rho_u)$ but keeps away from the boundaries and vice versa.

Throughout this paper, we select [49]

$$\eta(t)=\frac{\rho_l\rho_u\xi(t)}{(\rho_l+\xi(t))(\rho_u-\xi(t))}. \tag{7}$$

Remark 5. It follows from Remark 4 that $-\rho_l<\xi(0)<\rho_u$ holds naturally, which means that $\eta(t)$ is defined at $t=0$. On this basis, a careful inspection of (7) reveals that if $\eta(t)$ is bounded for all $t\geqslant 0$, then Eq. (6) is guaranteed. By this means, the problem of fast accurate reference tracking is converted into that of ensuring the boundedness of $\eta(t)$ for all $t\geqslant 0$.

Then, taking the time derivative of $\eta(t)$ yields

$$\dot{\eta}(t)=\mu(t)(\dot{x}_1(t)-\dot{y}_r(t)-\dot{\phi}(t)e(0)), \tag{8}$$

where $\mu(t)=\frac{\rho_l^2\rho_u^2+\rho_l\rho_u\xi^2(t)}{(\rho_l+\xi(t))^2(\rho_u-\xi(t))^2}>0$. For the notational simplicity, the time or state dependence of some variables may be omitted in the sequel. By replacing the equation of $\dot{x}_1$ with $\dot{\eta}$, Eq. (1) is transformed to

$$\begin{cases}\dot{\eta}=\mu(f_1+g_1x_2+d_1-\dot{y}_r-\dot{\phi}e(0)),\\ \dot{x}_i=f_i+g_ix_{i+1}+d_i,\quad i=2,\ldots,n-1,\\ \dot{x}_n=f_n+g_nu+d_n,\\ y=x_1.\end{cases} \tag{9}$$

3 Control design and performance analysis

In this section, a novel adaptive robust tracking control approach with tight performance guarantees is put forward to cope with Problem 1.

3.1 Adaptive PPC design

Different from the classical backstepping design [34, 35, 48], this paper introduces the dynamic surface control-based design philosophy [1, 2, 18, 19, 40–42] equipped with the following change of variables to address the problem of "explosion of complexity":

$$z_1 = \eta, \quad z_i = x_i - \alpha_{i,f}, \quad i = 2, \ldots, n \tag{10}$$

with $\alpha_{i,f}$, $i = 2, \ldots n$, denoting the outputs of the following first-order filters:

$$\varepsilon_i \dot{\alpha}_{i,f} = (\alpha_{i-1} - \alpha_{i,f})^3, \quad \alpha_{i,f}(0) = \alpha_{i-1}(0), \quad i = 2, \ldots, n, \tag{11}$$

where $\varepsilon_i > 0$, $i = 2, \ldots, n$ are design parameters, and α_{i-1}, $i = 2, \ldots, n$ stand for the virtual control laws which are regarded as the inputs of (11). Subsequently, the boundary layer errors are defined by

$$\varpi_i = \alpha_{i,f} - \alpha_{i-1}, \quad i = 2, \ldots, n. \tag{12}$$

For ease of notation [32], let $\theta = \max\{\delta_1^2, \ldots, \delta_n^2\}$ and $\beta = \max\{\beta_1, \ldots, \beta_n\}$, where the definitions of β_i, $i = 1, \ldots, n$, will be given shortly. Denote the estimates of θ and β as $\hat{\theta}$ and $\hat{\beta}$, respectively. Then, the corresponding estimation errors are $\tilde{\theta} = \theta - \hat{\theta}$ and $\tilde{\beta} = \beta - \hat{\beta}$. The controller design is conducted recursively.

Step 1. Through (10) and (12), we get

$$x_i = z_i + \varpi_i + \alpha_{i-1}, \quad i = 2, \ldots, n. \tag{13}$$

From (9), (10) and (13), the differential equation for z_1 is obtained by

$$\dot{z}_1 = \mu(f_1 + g_1(z_2 + \varpi_2 + \alpha_1) + d_1 - \dot{y}_r - \dot{\phi}e(0)). \tag{14}$$

Choose the Lyapunov function candidate as $V_1 = \frac{1}{2\underline{g}_1} z_1^2 + \frac{1}{2h}\tilde{\theta}^2 + \frac{1}{2\upsilon}\tilde{\beta}^2 + \frac{1}{2}\varpi_2^2$, where h and υ are positive design parameters. The time derivative of V_1 is computed by (14) as

$$\dot{V}_1 = \frac{g_1}{\underline{g}_1}\mu z_1 z_2 + \frac{1}{\underline{g}_1}\mu z_1(f_1 + g_1\varpi_2 + g_1\alpha_1 + d_1 - \dot{y}_r - \dot{\phi}e(0)) - \frac{1}{h}\tilde{\theta}\dot{\hat{\theta}} - \frac{1}{\upsilon}\tilde{\beta}\dot{\hat{\beta}} + \varpi_2\dot{\varpi}_2. \tag{15}$$

Subsequently, invoking Young's inequality, Assumptions 1–3 and Lemma 1, we have

$$\frac{g_1}{\underline{g}_1}\mu z_1 z_2 \leqslant \mu^2 z_1^2 z_2^2 + \frac{\overline{g}_1^2}{4\underline{g}_1^2}, \quad \frac{1}{\underline{g}_1}\mu z_1 f_1 \leqslant \mu^2 z_1^2 \delta_1^2 \Psi_1^2 + \frac{1}{4\underline{g}_1^2} \leqslant \mu^2 z_1^2 \Psi_1^2 \theta + \frac{1}{4\underline{g}_1^2}, \tag{16}$$

$$\frac{g_1}{\underline{g}_1}\mu z_1 \varpi_2 \leqslant \mu^2 z_1^2 + \frac{1}{4}\varpi_2^4 + \frac{\overline{g}_1^4}{16\underline{g}_1^4}, \quad \mu z_1 \frac{d_1}{\underline{g}_1} \leqslant \mu |z_1| \beta_1 < \frac{2}{\pi}\mu z_1 \beta \arctan\left(\frac{\mu z_1}{\sigma_1}\right) + \frac{2}{\pi}\beta\sigma_1, \tag{17}$$

$$-\frac{1}{\underline{g}_1}\mu z_1 \dot{y}_r \leqslant \mu^2 z_1^2 \dot{y}_r^2 + \frac{1}{4\underline{g}_1^2}, \quad -\frac{1}{\underline{g}_1}\mu z_1 \dot{\phi} e(0) \leqslant \mu^2 z_1^2 \dot{\phi}^2 e^2(0) + \frac{1}{4\underline{g}_1^2}, \tag{18}$$

where $\sigma_1 > 0$ is a design parameter, and $\beta_1 = \frac{\overline{d}_1}{\underline{g}_1}$. Adding both sides of (16)–(18), we further have

$$\frac{1}{\underline{g}_1} z_1 \dot{z}_1 \leqslant \mu^2 z_1^2 z_2^2 + \frac{g_1}{\underline{g}_1}\mu z_1 \alpha_1 + z_1 \Phi_1 + \mu^2 z_1^2 \Psi_1^2 \tilde{\theta} + \frac{2}{\pi}\mu z_1 \tilde{\beta} \arctan\left(\frac{\mu z_1}{\sigma_1}\right) + \frac{1}{4}\varpi_2^4 + \Pi_1, \tag{19}$$

where $\Phi_1 = \mu^2 z_1 \Psi_1^2 \hat{\theta} + \frac{2}{\pi}\mu\hat{\beta}\arctan(\frac{\mu z_1}{\sigma_1}) + \mu^2 z_1 + \mu^2 z_1 \dot{y}_r^2 + \mu^2 z_1 \dot{\phi}^2 e^2(0)$ and $\Pi_1 = \frac{2}{\pi}\beta\sigma_1 + \frac{\overline{g}_1^2}{4\underline{g}_1^2} + \frac{\overline{g}_1^4}{16\underline{g}_1^4} + \frac{3}{4\underline{g}_1^2}$. Then, the virtual control law, α_1, is given by

$$\alpha_1 = -\frac{1}{\mu}(k_1 z_1 + \Phi_1), \tag{20}$$

where $k_1 > 0$ is a design parameter. Putting (19) and (20) into (15) leads to

$$\dot{V}_1 \leqslant \mu^2 z_1^2 z_2^2 - k_1 z_1^2 + \frac{1}{h}\tilde{\theta}\left(\tau_{1,1} - \dot{\hat{\theta}}\right) + \frac{1}{\upsilon}\tilde{\beta}\left(\tau_{1,2} - \dot{\hat{\beta}}\right) + \frac{1}{4}\varpi_2^4 + \varpi_2\dot{\varpi}_2 + \Pi_1, \tag{21}$$

where $\tau_{1,1} = h\mu^2 z_1^2 \Psi_1^2$ and $\tau_{1,2} = \frac{2}{\pi}\upsilon\mu z_1 \arctan(\frac{\mu z_1}{\sigma_1})$. By (11) and (12), there holds $\dot{\varpi}_2 = -\frac{\varpi_2^3}{\varepsilon_2} - \dot{\alpha}_1$ with $\dot{\alpha}_1 = \frac{\partial \alpha_1}{\partial z_1}\dot{z}_1 + \frac{\partial \alpha_1}{\partial \mu}\dot{\mu} + \frac{\partial \alpha_1}{\partial \Phi_1}\dot{\Phi}_1$. Let $\Lambda_1 = \dot{\alpha}_1$. Then, we get $\frac{1}{4}\varpi_2^4 + \varpi_2\dot{\varpi}_2 = \frac{1}{4}\varpi_2^4 - \frac{1}{\varepsilon_2}\varpi_2^4 - \varpi_2\Lambda_1 \leqslant (\frac{1}{2} - \frac{1}{\varepsilon_2})\varpi_2^4 + \frac{1}{2}\Lambda_1^2 + \frac{1}{4}$. Substituting it into (21) and choosing $0 < \varepsilon_2 < 1/(\frac{1}{2} + c_2)$ with $c_2 > 0$ being a constant yield

$$\dot{V}_1 \leqslant \mu^2 z_1^2 z_2^2 - k_1 z_1^2 + \frac{1}{h}\tilde{\theta}\left(\tau_{1,1} - \dot{\hat{\theta}}\right) + \frac{1}{\upsilon}\tilde{\beta}\left(\tau_{1,2} - \dot{\hat{\beta}}\right) - c_2\varpi_2^4 + \frac{1}{2}\Lambda_1^2 + \Gamma_1, \quad \Gamma_1 = \Pi_1 + \frac{1}{4}. \tag{22}$$

Step i $(i = 2, \ldots, n-1)$**.** Computing the time derivative of $\frac{1}{2\underline{g}_i}z_i^2$ by using (9), (10) and (13) leads to $\frac{1}{\underline{g}_i}z_i\dot{z}_i = \frac{1}{\underline{g}_i}z_i(f_i + g_i z_{i+1} + g_i\varpi_{i+1} + g_i\alpha_i + d_i - \dot{\alpha}_{i,f})$. Similarly to Step 1, by Young's inequality, Assumptions 1–3 and Lemma 1, there hold

$$\begin{aligned}
&\frac{1}{\underline{g}_i}z_i f_i \leqslant z_i^2\Psi_i^2\theta + \frac{1}{4\underline{g}_i^2}, \quad \frac{g_i}{\underline{g}_i}z_i z_{i+1} \leqslant z_i^2 z_{i+1}^2 + \frac{\overline{g}_i^2}{4\underline{g}_i^2}, \quad \frac{g_i}{\underline{g}_i}z_i\varpi_{i+1} \leqslant z_i^2 + \frac{1}{4}\varpi_{i+1}^4 + \frac{\overline{g}_i^4}{16\underline{g}_i^4},\\
&z_i\frac{d_i}{\underline{g}_i} \leqslant |z_i|\beta_i < \frac{2}{\pi}z_i\beta\arctan\left(\frac{z_i}{\sigma_i}\right) + \frac{2}{\pi}\beta\sigma_i, \quad -\frac{1}{\underline{g}_i}z_i\dot{\alpha}_{i,f} \leqslant z_i^2\dot{\alpha}_{i,f}^2 + \frac{1}{4\underline{g}_i^2},
\end{aligned}$$

where σ_i is a positive design parameter, and $\beta_i = \frac{\overline{d}_i}{\underline{g}_i}$. Further, we can obtain

$$\frac{1}{\underline{g}_i}z_i\dot{z}_i \leqslant z_i^2 z_{i+1}^2 + \frac{g_i}{\underline{g}_i}z_i\alpha_i + z_i\Phi_i + z_i^2\Psi_i^2\tilde{\theta} + \frac{2}{\pi}z_i\tilde{\beta}\arctan\left(\frac{z_i}{\sigma_i}\right) + \frac{1}{4}\varpi_{i+1}^4 + \Pi_i, \tag{23}$$

where $\Phi_i = z_i\Psi_i^2\hat{\theta} + \frac{2}{\pi}\hat{\beta}\arctan(\frac{z_i}{\sigma_i}) + z_i + z_i\dot{\alpha}_{i,f}^2$ and $\Pi_i = \frac{2}{\pi}\beta\sigma_i + \frac{\overline{g}_i^2}{4\underline{g}_i^2} + \frac{\overline{g}_i^4}{16\underline{g}_i^4} + \frac{1}{2\underline{g}_i^2}$. Then, the virtual control laws, α_i, $i = 2, \ldots, n-1$, are designed by

$$\alpha_2 = -\left(k_2 z_2 + \mu^2 z_1^2 z_2 + \Phi_2\right), \tag{24}$$

$$\alpha_i = -\left(k_i z_i + z_{i-1}^2 z_i + \Phi_i\right), \quad i = 3, \ldots, n-1, \tag{25}$$

where k_i, $i = 2, \ldots, n-1$, are positive design parameters. Consider the Lyapunov function candidate as $V_i = V_{i-1} + \frac{1}{2\underline{g}_i}z_i^2 + \frac{1}{2}\varpi_{i+1}^2$. This in conjunction with (22)–(25) gives

$$\begin{aligned}
\dot{V}_i \leqslant& z_i^2 z_{i+1}^2 - \sum_{j=1}^{i} k_j z_j^2 + \frac{1}{h}\tilde{\theta}\left(\tau_{i,1} - \dot{\hat{\theta}}\right) + \frac{1}{\upsilon}\tilde{\beta}\left(\tau_{i,2} - \dot{\hat{\beta}}\right) + \Pi_i\\
&+ \frac{1}{4}\varpi_{i+1}^4 + \varpi_{i+1}\dot{\varpi}_{i+1} - \sum_{j=1}^{i-1} c_{j+1}\varpi_{j+1}^4 + \sum_{j=1}^{i-1}\frac{1}{2}\Lambda_j^2 + \sum_{j=1}^{i-1}\Gamma_j,
\end{aligned} \tag{26}$$

where $\tau_{i,1} = \tau_{i-1,1} + h z_i^2\Psi_i^2$ and $\tau_{i,2} = \tau_{i-1,2} + \frac{2}{\pi}\upsilon z_i\arctan(\frac{z_i}{\sigma_i})$. Note from (11) and (12) that $\dot{\varpi}_{i+1} = -\frac{\varpi_{i+1}^3}{\varepsilon_{i+1}} - \dot{\alpha}_i$, $i = 2, \ldots, n-1$, where $\dot{\alpha}_2 = \frac{\partial \alpha_2}{\partial z_1}\dot{z}_1 + \frac{\partial \alpha_2}{\partial z_2}\dot{z}_2 + \frac{\partial \alpha_2}{\partial \mu}\dot{\mu} + \frac{\partial \alpha_2}{\partial \Phi_2}\dot{\Phi}_2$ and $\dot{\alpha}_i = \frac{\partial \alpha_i}{\partial z_{i-1}}\dot{z}_{i-1} + \frac{\partial \alpha_i}{\partial z_i}\dot{z}_i + \frac{\partial \alpha_i}{\partial \Phi_i}\dot{\Phi}_i$, $i = 3, \ldots, n-1$. Further, it can be derived that $\frac{1}{4}\varpi_{i+1}^4 + \varpi_{i+1}\dot{\varpi}_{i+1} \leqslant (\frac{1}{2} - \frac{1}{\varepsilon_{i+1}})\varpi_{i+1}^4 + \frac{1}{2}\Lambda_i^2 + \frac{1}{4}$ with $\Lambda_i = \dot{\alpha}_i$. Inserting the above inequality into (26) and letting $0 < \varepsilon_{i+1} < 1/(\frac{1}{2} + c_{i+1})$ with $c_{i+1} > 0$ being a constant yield

$$\dot{V}_i \leqslant z_i^2 z_{i+1}^2 - \sum_{j=1}^{i} k_j z_j^2 + \frac{1}{h}\tilde{\theta}(\tau_{i,1} - \dot{\hat{\theta}}) + \frac{1}{\upsilon}\tilde{\beta}(\tau_{i,2} - \dot{\hat{\beta}}) - \sum_{j=1}^{i} c_{j+1}\varpi_{j+1}^4 + \sum_{j=1}^{i}\frac{1}{2}\Lambda_j^2 + \sum_{j=1}^{i}\Gamma_j, \tag{27}$$

where $\Gamma_i = \Pi_i + \frac{1}{4}$.

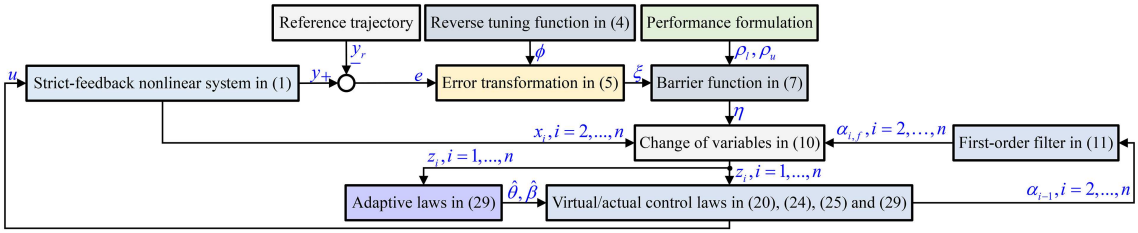

Figure 3 (Color online) Schematic of the proposed adaptive PPC architecture.

Step n**.** At this step, it is noted from (9) and (10) that $\frac{1}{\underline{g}_n} z_n \dot{z}_n = \frac{1}{\underline{g}_n} z_n (f_n + g_n u + d_n - \dot{\alpha}_{n,f})$. Following the same line as in Step i, we can derive $\frac{1}{\underline{g}_n} z_n \dot{z}_n \leqslant \frac{g_n}{\underline{g}_n} z_n u + z_n \Phi_n + z_n^2 \Psi_n^2 \tilde{\theta} + \frac{2}{\pi} z_n \tilde{\beta} \arctan(\frac{z_n}{\sigma_n}) + \Pi_n$, where $\Phi_n = z_n \Psi_n^2 \hat{\theta} + \frac{2}{\pi} \hat{\beta} \arctan(\frac{z_n}{\sigma_n}) + z_n \dot{\alpha}_{n,f}^2$ and $\Pi_n = \frac{2}{\pi} \beta \sigma_n + \frac{1}{2\underline{g}_n^2}$ with $\sigma_n > 0$ and $\beta_n = \frac{\overline{d}_n}{\underline{g}_n}$. Construct the Lyapunov function candidate as $V_n = V_{n-1} + \frac{1}{2\underline{g}_n} z_n^2$, which, together with (27) for $i = n-1$, yields

$$\begin{aligned} \dot{V}_n \leqslant & \frac{g_n}{\underline{g}_n} z_n u + z_n \left(z_{n-1}^2 z_n + \Phi_n \right) + \Pi_n - \sum_{j=1}^{n-1} k_j z_j^2 + \frac{1}{h} \tilde{\theta} \left(\tau_{n,1} - \dot{\hat{\theta}} \right) \\ & + \frac{1}{\upsilon} \tilde{\beta} \left(\tau_{n,2} - \dot{\hat{\beta}} \right) - \sum_{j=1}^{n-1} c_{j+1} \varpi_{j+1}^4 + \sum_{j=1}^{n-1} \frac{1}{2} \Lambda_j^2 + \sum_{j=1}^{n-1} \Gamma_j, \end{aligned} \tag{28}$$

where $\tau_{n,1} = \tau_{n-1,1} + h z_n^2 \Psi_n^2$ and $\tau_{n,2} = \tau_{n-1,2} + \frac{2}{\pi} \upsilon z_n \arctan(\frac{z_n}{\sigma_n})$. The actual control law, u, and the update laws for $\hat{\theta}$ and $\hat{\beta}$ are severally designed as follows:

$$\begin{cases} u = -\left(k_n z_n + z_{n-1}^2 z_n + \Phi_n \right), \\ \dot{\hat{\theta}} = \tau_{n,1} - l\hat{\theta}, \quad \hat{\theta}(0) \geqslant 0, \\ \dot{\hat{\beta}} = \tau_{n,2} - m\hat{\beta}, \quad \hat{\beta}(0) \geqslant 0, \end{cases} \tag{29}$$

where k_n, l, and m are positive design parameters. Inserting (29) into (28) leads to

$$\dot{V}_n \leqslant -\sum_{j=1}^{n} k_j z_j^2 + \frac{l}{h} \tilde{\theta} \hat{\theta} + \frac{m}{\upsilon} \tilde{\beta} \hat{\beta} - \sum_{j=1}^{n-1} c_{j+1} \varpi_{j+1}^4 + \sum_{j=1}^{n-1} \frac{1}{2} \Lambda_j^2 + \sum_{j=1}^{n-1} \Gamma_j + \Pi_n. \tag{30}$$

A schematic of the proposed adaptive PPC architecture is exhibited in Figure 3.

3.2 Performance analysis

The theoretical result of this paper is stated as follows.

Theorem 1. If Assumptions 1–4 hold, then Problem 1 is solved by the control scheme in (4), (5), (7), (10), (11), (20), (24), (25) and (29) under any known initial condition.

Proof. Due to $\varpi_{j+1}^2 \leqslant \varpi_{j+1}^4 + \frac{1}{4}$, $j = 1, \ldots, n-1$, $\tilde{\theta}\hat{\theta} \leqslant -\frac{1}{2}\tilde{\theta}^2 + \frac{1}{2}\theta^2$, and $\tilde{\beta}\hat{\beta} \leqslant -\frac{1}{2}\tilde{\beta}^2 + \frac{1}{2}\beta^2$, Eq. (30) is further scaled by

$$\dot{V}_n \leqslant -\sum_{j=1}^{n} k_j z_j^2 - \frac{l}{2h} \tilde{\theta}^2 - \frac{m}{2\upsilon} \tilde{\beta}^2 - \sum_{j=1}^{n-1} c_{j+1} \varpi_{j+1}^2 + \frac{l}{2h} \theta^2 + \frac{m}{2\upsilon} \beta^2 + \sum_{j=1}^{n-1} \frac{1}{4} c_{j+1} + \sum_{j=1}^{n-1} \frac{1}{2} \Lambda_j^2 + \sum_{j=1}^{n-1} \Gamma_j + \Pi_n.$$

In view of [1, 2, 18, 19, 40–42], consider the compact set $\Omega_V := \{\sum_{j=1}^{n} \frac{1}{\underline{g}_j} z_j^2 + \frac{1}{h}\tilde{\theta}^2 + \frac{1}{\upsilon}\tilde{\beta}^2 + \sum_{j=2}^{n} \varpi_j^2 \leqslant 2B_0\} \subset \mathbb{R}^{2n+1}$ with $B_0 > 0$. Consequently, there exists a positive constant, M_i, such that $|\Lambda_i| \leqslant M_i$ on Ω_V, $i = 1, \ldots, n-1$. Then, there holds

$$\dot{V}_n \leqslant -\sum_{j=1}^{n} k_j z_j^2 - \frac{l}{2h} \tilde{\theta}^2 - \frac{m}{2\upsilon} \tilde{\beta}^2 - \sum_{j=2}^{n} c_j \varpi_j^2 + \Gamma \leqslant -\Upsilon V_n + \Gamma, \tag{31}$$

where $\Upsilon = \min\{2k_j\underline{g}_j, l, m, 2c_k\} > 0$, $j = 1, \ldots, n$, $k = 2, \ldots, n$, and $\Gamma = \frac{l}{2h}\theta^2 + \frac{m}{2\upsilon}\beta^2 + \sum_{j=2}^{n}\frac{1}{4}c_j + \sum_{j=1}^{n-1}\frac{1}{2}M_j^2 + \sum_{j=1}^{n-1}\Gamma_j + \Pi_n > 0$.

Proceed with verifying the uniform boundedness of all the signals in the control system. The inequality in (31) implies that $\dot{V}_n < 0$ on $V_n = B_0$ when $\Upsilon > \frac{\Gamma}{B_0}$. Accordingly, $V_n \leqslant B_0$ is an invariant set, i.e., if $V_n(0) \leqslant B_0$, then $V_n \leqslant B_0$ for all $t \geqslant 0$. This implies that the uniform boundedness of z_i, $i = 1, \ldots, n$, $\tilde{\theta}$, $\tilde{\beta}$, and ϖ_i, $i = 2, \ldots, n$, is ensured. Invoking $\tilde{\theta} = \theta - \hat{\theta}$ and $\tilde{\beta} = \beta - \hat{\beta}$, we obtain $\hat{\theta} \in \mathcal{L}^\infty$ and $\hat{\beta} \in \mathcal{L}^\infty$. Due to $z_1 = \eta \in \mathcal{L}^\infty$, it follows from (7), Remark 5 and (8) that $-\rho_l < \xi < \rho_u$ for all $t \geqslant 0$ and $\mu \in \mathcal{L}^\infty$. Note from Assumption 4 and (4) that $y_r \in \mathcal{L}^\infty$, $\dot{y}_r \in \mathcal{L}^\infty$, $\phi \in \mathcal{L}^\infty$, and $\dot{\phi} \in \mathcal{L}^\infty$. By (5), there holds $x_1 \in \mathcal{L}^\infty$. This together with the continuity of $\Psi_1(\overline{x}_1)$ in Assumption 1 with respect to $\overline{x}_1$ (i.e., x_1) yields the uniform boundedness of $\Psi_1(\overline{x}_1)$. The above facts along with (20) guarantee $\alpha_1 \in \mathcal{L}^\infty$. Therefore, x_2 in (13) is uniformly bounded. Take the same way to evaluate $\alpha_2, \ldots, \alpha_{n-1}$, $x_3, \ldots, x_n$, and u. Then, it can be deduced that $\alpha_i \in \mathcal{L}^\infty$, $i = 2, \ldots, n-1$, $x_i \in \mathcal{L}^\infty$, $i = 3, \ldots, n$, and $u \in \mathcal{L}^\infty$. Further, $\alpha_{i,f}$ in (12) is uniformly bounded, $i = 2, \ldots, n$.

What remains to be analyzed is the tracking performance of the control system. Applying $-\rho_l < \xi < \rho_u$ for all $t \geqslant 0$ to Remark 4 shows that the quantitative regulation of the behavior of the tracking error on $[0, T_f)$ is achieved and the performance requirement in (3) is fulfilled.

Remark 6. Both the FC method and the PPC method can be employed to achieve reference tracking with the prescribed transient and steady-state behavior. FC is a continuation of the adaptive high-gain control methodology, where the monotonically increasing control gain is replaced with a time-varying and error-dependent function. In this direction, the controller design is conducted based on a pivotal component, which is composed of the gain function multiplying the tracking error, in the form of $\eta_{\mathrm{FC}}(t) = \frac{1}{1-\frac{|e(t)|}{\rho(t)}}e(t)$ [8]. By contrast, the key idea in PPC is the introduction of an error transformation incorporating the desired performance specifications to yield the transformed system of the original controlled system, where the error transformation function is commonly chosen as $\eta_{\mathrm{PPC},1}(t) = \ln\left(\frac{\rho(t)+e(t)}{\rho(t)-e(t)}\right)$ [15]. Nevertheless, it is noteworthy that there exists a non-differentiable problem of $|e(t)|$ with $e(t) = 0$ in $\eta_{\mathrm{FC}}(t)$. Although the improved work [20] was conducted to avoid this problem, it fails to handle the asymmetric constraint in (6) straightforwardly, e.g., the overshoot. On the contrary, such a specification can be directly introduced by $\eta_{\mathrm{PPC},2}(t) = \ln\left(\frac{\rho(t)+e(t)}{\overline{\rho}(t)-e(t)}\right)$. As a matter of fact, $\eta_{\mathrm{FC}}(t)$, $\eta_{\mathrm{PPC},1}(t)$ and $\eta_{\mathrm{PPC},2}(t)$ all belong to barrier functions, and Eq. (6) is an error constraint in essence. In addition to $\eta_{\mathrm{PPC},2}(t)$, other types of barrier functions are also feasible to ensure (6) as long as they own the infinity property, e.g., (7) in this paper and (15) in [22]. Accordingly, Problem 1 is solved by the barrier function-based constrained control method within the robust adaptive control framework.

Remark 7. Instead of the tuning function-based initialization technique [22,23], the performance funnel with an infinitely large entry [24–32], and the exponential function related to the initial tracking error [37], the reverse tuning function in (4) is adopted to adjust the tracking error, and then the performance constraint is imposed on the adjusted error, i.e., (6) with (5). By this means, reference tracking with the predefined transient and steady-state performance specifications on the overshoot, the settling time and the accuracy is achieved while ensuring the natural satisfaction of the initial condition. Nonetheless, it is noteworthy that due to the error transformation in (5), the known initial tracking error is required for the online control design, rendering the off-line control design infeasible. On the other hand, in practical application, strict performance specifications are generally effective in regulating the transient and steady-state behavior of the tracking error. In the case of low-frequency sampling of the computer control system, nevertheless, such specifications may be adverse when a disturbance with a large amplitude of change is present. This is because the violent variation of the tracking error results in the highly possible appearance of constraint violation. In this direction, the following example is illustrative.

Example 1. Consider the longitudinal vehicle system [27], $\dot{p} = \vartheta + d_1(t)$, $M\dot{\vartheta} = f(\vartheta) + u + d_2(t)$, where $M = 50$, p and ϑ are the mass, position and velocity of the vehicle, respectively; u is the control input; $f(\vartheta) = -50\vartheta - 25|\vartheta|\vartheta$ denotes the aerodynamic friction; $d_1(t)$ shown in Figure 4(c) and $d_2(t) = 0.05\sin(0.1t)$ stand for the exogenous disturbances. The control objective is to steer $p(t)$ to track $y_r(t) = \sin(0.2t)$ with $|p(t) - y_r(t)| < 0.05$, $t \geqslant 3$. Following Theorem 1, a controller is formed with $T_f = 3$, $\lambda = 1$, $\rho_l = 0.05$, $\rho_u = 0.05$, $k_1 = 20$, $\sigma_1 = 0.02$, $k_2 = 200$, $\sigma_2 = 0.02$, $\varepsilon_1 = 0.001$, $h = 5$, $l = 20$, $\upsilon = 1$, $m = 3$, and $\Psi(\vartheta) = (\vartheta - 1)^2$. In the simulation, let $p(0) = 1$, $\vartheta(0) = 0$, $\hat{\theta}(0) = 0$, and $\hat{\beta}(0) = 0$. The simulation is conducted under MATLAB with the 0.0 start time, the 10 stop time, and the fixed-step type. Apply

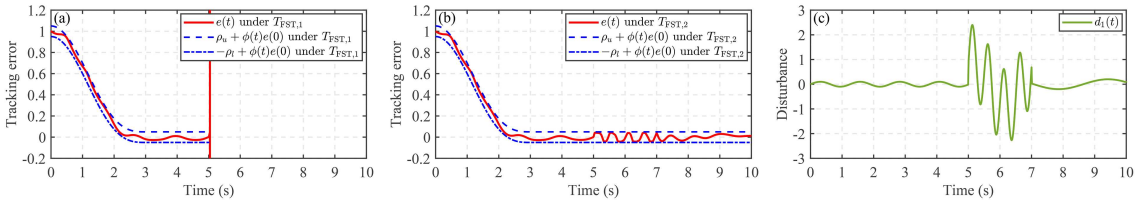

Figure 4 (Color online) Evolutions of the tracking errors under the different FSTs and the disturbance. (a) The tracking error and performance envelope under $T_{\mathrm{FST},1}=0.001$; (b) the tracking error and performance envelope under $T_{\mathrm{FST},2}=0.0001$; (c) the disturbance $d_1(t)$.

the controller to the longitudinal vehicle system and set the different fundamental sample times (FSTs), i.e., $T_{\mathrm{FST},1}=0.001$ and $T_{\mathrm{FST},2}=0.0001$. The simulation results are exhibited in Figures 4(a) and (b). It is seen from Figure 4(a) with $T_{\mathrm{FST},1}=0.001$ that fast accurate reference tracking with the small error overshoot is realized before $t=5$. After the abrupt change in the amplitude of $d_1(t)$, nevertheless, the tracking error shows frequent fluctuation such that it violates the prescribed performance constraint, and even the system loses control. In contrast, the controller under $T_{\mathrm{FST},2}=0.0001$ works well for this case; see Figure 4(b). However, this is highly dependent on the sampling frequency of the practical control system and is at the cost of increasing the computation burden in control implementation. Therefore, motivated by the above technical challenges, a solution capable of enhancing the reliability of control implementation under low-frequency sampling is given in Section 4.

4 Extension to self-adjustable performance constraint

The technical development conducted in the previous sections is extended to a more general case with the self-adjustable performance constraint in this section. A way to strengthen the reliability of control designs is provided by appropriately relaxing the performance specifications and adapting the control gain such that the tracking task is successfully implemented in the presence of paroxysmal factors.

4.1 Problem statement

The problem treated in this section reads as follows.

Problem 2. For the strict-feedback system in (1) under the disturbances with large amplitude of change, develop a robust controller such that (P1) the reliability of the control system is enhanced; (P2) all the signals involved in the closed loop are bounded; (P3) the evolution of the tracking error over time satisfies

$$\phi(t)e(0)-\rho_l(t)-\omega_l(t)<e(t)<\phi(t)e(0)+\rho_u(t)+\omega_u(t),\quad \forall t\geqslant 0. \tag{32}$$

Here, $\phi(t)$ is given in (4); $\tilde{\rho}<\rho_l(t)<\infty$ and $\tilde{\rho}<\rho_u(t)<\infty$ with $\tilde{\rho}$ being a positive constant; the modification signals, $\omega_l(t)$ and $\omega_u(t)$, are given by

$$\omega_i(t)=\frac{2}{\pi}(p_{1,i}+\hat{\beta}_1(t))\arctan(\Delta_i(t)),\quad i\in\{l,u\}, \tag{33}$$

where $p_{1,l}$ and $p_{1,u}$ are positive constants; $\hat{\beta}_1(t)\in\mathbb{R}_{\geqslant 0}$ will be designed later soon in (40); $\Delta_l(t)\in\mathbb{R}_{\geqslant 0}$ and $\Delta_u(t)\in\mathbb{R}_{\geqslant 0}$ are generated by the following user-appointed degradation rules:

$$\begin{cases}\dot{\Delta}_l(t)=-p_{2,l}\Delta_l(t)+p_{3,l}^3\delta_l(t),\\ \delta_l(t)=(\mathrm{sign}\,(e(t)-\phi(t)e(0)+p_{4,l}\rho_l(t))-1)\,(e(t)-\phi(t)e(0)+p_{4,l}\rho_l(t))^3,\end{cases} \tag{34}$$

$$\begin{cases}\dot{\Delta}_u(t)=-p_{2,u}\Delta_u(t)+p_{3,u}^3\delta_u(t),\\ \delta_u(t)=(\mathrm{sign}\,(e(t)-\phi(t)e(0)-p_{4,u}\rho_u(t))+1)\,(e(t)-\phi(t)e(0)-p_{4,u}\rho_u(t))^3,\end{cases} \tag{35}$$

with $\Delta_l(0)=0$ and $\Delta_u(0)=0$, where $p_{2,i}>0$, $p_{3,i}>0$, and $0<p_{4,i}<1$ are design parameters, $i\in\{l,u\}$; $(\phi(t)e(0)-p_{4,l}\rho_l(t))$ and $(\phi(t)e(0)+p_{4,u}\rho_u(t))$ denote the monitoring functions (MFs) inside the performance envelope; $\mathrm{sign}(\cdot)$ represents the signum function [29, 43].

Table 1 Values of $\delta_l(t)$ and $\delta_u(t)$ based on the relationship between the tracking error and the MFs.

Relationship between the tracking error and the MFs	$\delta_l(t)$	$\delta_u(t)$
$e(t) < (\phi(t)e(0) - p_{4,l}\rho_l(t))$	$-2(e(t) - \phi(t)e(0) + p_{4,l}\rho_l(t))^3 > 0$	0
$(\phi(t)e(0) - p_{4,l}\rho_l(t)) \leqslant e(t) \leqslant (\phi(t)e(0) + p_{4,u}\rho_u(t))$	0	0
$e(t) > (\phi(t)e(0) + p_{4,u}\rho_u(t))$	0	$2(e(t) - \phi(t)e(0) - p_{4,u}\rho_u(t))^3 > 0$

Remark 8. It is seen from (34) and (35) that the values of $\delta_l(t)$ and $\delta_u(t)$ depend on the relationship between $e(t)$, $(\phi(t)e(0) - p_{4,l}\rho_l(t))$, and $(\phi(t)e(0) + p_{4,u}\rho_u(t))$; see Table 1 for details. It is not difficult to verify that $\delta_l(t)$ and $\delta_u(t)$ are continuous and differentiable in time, despite the involvement of the signum function in (34) and (35). Due to $\delta_l(t) \geqslant 0$ and $\delta_u(t) \geqslant 0$, we obtain from Lemma 2 that $\Delta_l(t)$ and $\Delta_u(t)$ are nonnegative under $\Delta_l(0) = \Delta_u(0) = 0$. They together with $\hat{\beta}_1(t) \geqslant 0$ are supplied to (33), further acquiring the modified performance boundaries $(\phi(t)e(0) - \rho_l(t) - \omega_l(t))$ and $(\phi(t)e(0) + \rho_u(t) + \omega_u(t))$. Moreover, $p_{4,l}$ and $p_{4,u}$ play the role of the ratio thresholds. If $e(t)$ evolves inside the prespecified "safe region", i.e., $[\phi(t)e(0) - p_{4,l}\rho_l(t), \phi(t)e(0) + p_{4,u}\rho_u(t)]$, then by (34) and (35), $\omega_l(t)$ and $\omega_u(t)$ are equal to zero, and the performance boundaries on $e(t)$ are maintained in the original forms, i.e., $(\phi(t)e(0) - \rho_l(t))$ and $(\phi(t)e(0) + \rho_u(t))$. In this case, there is no need to modify the performance boundaries on $e(t)$ and to relax the performance specifications. If $e(t)$ is outside $[\phi(t)e(0) - p_{4,l}\rho_l(t), \phi(t)e(0) + p_{4,u}\rho_u(t)]$, then the performance boundaries on $e(t)$ are automatically modified from $(\phi(t)e(0) - \rho_l(t))$ and $(\phi(t)e(0) + \rho_u(t))$ to $(\phi(t)e(0) - \rho_l(t) - \omega_l(t))$ and $(\phi(t)e(0) + \rho_u(t) + \omega_u(t))$ accordingly. Once $e(t)$ reenters into $[\phi(t)e(0) - p_{4,l}\rho_l(t), \phi(t)e(0) + p_{4,u}\rho_u(t)]$, $(\phi(t)e(0) - \rho_l(t) - \omega_l(t))$ and $(\phi(t)e(0) + \rho_u(t) + \omega_u(t))$ will converge to $(\phi(t)e(0) - \rho_l(t))$ and $(\phi(t)e(0) + \rho_u(t))$ exponentially fast, respectively, with the convergence rate governed by $p_{2,l}$ and $p_{2,u}$. The above analysis implies that the modification scheme in (32)–(35) is crucial in avoiding violation of the performance constraint and enhancing the reliability of control implementation, as we will prove below. On the other hand, the typical selections of $\rho_l(t)$ and $\rho_u(t)$ include but are not limited to the following functions:

$$\rho_i(t) = \rho_{i,0}\mathrm{e}^{-\ell_i t} + \rho_{i,\infty} \quad \text{and} \quad \rho_i(t) = \begin{cases} \rho_{i,0}\left(\frac{1}{2}\cos\left(\frac{\pi t}{\tilde{T}_i}\right) + \frac{1}{2}\right)^{\ell_i+2} + \rho_{i,\tilde{T}}, & \text{if } 0 \leqslant t < \tilde{T}_i, \\ \rho_{i,\tilde{T}}, & \text{otherwise,} \end{cases}$$

for each $i \in \{l, u\}$, where $\rho_{i,0}$, $\rho_{i,\infty}$, ℓ_i, $\tilde{T}_i$, and $\rho_{i,\tilde{T}}$ are positive constants, $i \in \{l, u\}$.

A lemma, which facilitates the upcoming control design, is provided below.

Lemma 3. Let $F_l(t) = \rho_l(t) + \omega_l(t)$ and $F_u(t) = \rho_u(t) + \omega_u(t)$, and then by (5), Eq. (32) is equivalent to

$$-F_l(t) < \xi(t) < F_u(t), \quad \forall t \geqslant 0. \tag{36}$$

Proof. It is straightforward and thus omitted.

4.2 Barrier function

With the aim at (36), the barrier function in (7) is modified to

$$\eta(t) = \frac{F_l(t)F_u(t)\xi(t)}{(F_l(t) + \xi(t))(F_u(t) - \xi(t))}. \tag{37}$$

From (5) and (37), the differential equation for $\eta(t)$ is obtained by

$$\dot{\eta}(t) = \mu_1(t)(\dot{x}_1(t) - \dot{y}_r(t) - \dot{\phi}(t)e(0)) + \mu_2(t), \tag{38}$$

where

$$\mu_1(t) = \frac{F_l^2(t)F_u^2(t) + F_l(t)F_u(t)\xi^2(t)}{(F_l(t) + \xi(t))^2(F_u(t) - \xi(t))^2} > 0,$$

$$\mu_2(t) = \frac{\xi^2(t)}{(F_l(t) + \xi(t))^2(F_u(t) - \xi(t))^2}(\dot{F}_l(t)F_u^2(t) - F_l^2(t)\dot{F}_u(t) - (F_l(t)\dot{F}_u(t) + \dot{F}_l(t)F_u(t))\xi(t)).$$

4.3 Self-adjustable performance-based control design

To deal with Problem 2, a self-adjustable performance-based adaptive robust control approach is proposed in this subsection. The controller design begins with the following change of variables:

$$z_1 = \eta, \quad z_i = x_i - \alpha_{i,f}, \quad i = 2, \ldots, n, \tag{39}$$

where $\alpha_{i,f}$ is obtained through (11). Subsequently, the controller design is conducted step by step.

Step 1. Differentiating z_1 in (39) by (1) and (38) yields $\dot{z}_1 = \mu_1(f_1 + g_1 x_2 + d_1 - \dot{y}_r - \dot{\phi}e(0)) + \mu_2$. Substituting (13) into the above equation, we have $\dot{z}_1 = \mu_1(f_1 + g_1(z_2 + \varpi_2 + \alpha_1) + d_1 - \dot{y}_r - \dot{\phi}e(0)) + \mu_2$. Choose the Lyapunov function candidate as $V_1 = \frac{1}{2\underline{g}_1}z_1^2 + \frac{1}{2h_1}\tilde{\theta}_1^2 + \frac{1}{2\upsilon_1}\tilde{\beta}_1^2 + \frac{1}{2}\varpi_2^2$, where h_1 and υ_1 are positive parameters; $\tilde{\theta}_1 = \theta_1 - \hat{\theta}_1$ and $\tilde{\beta}_1 = \beta_1 - \hat{\beta}_1$; $\hat{\theta}_1$ and $\hat{\beta}_1$ are the estimates of $\theta_1 = \delta_1^2$ and $\beta_1 = \frac{\overline{d}_1}{\underline{g}_1}$, respectively. Computing the time derivative of V_1 gives $\dot{V}_1 = \frac{g_1}{\underline{g}_1}\mu_1 z_1 z_2 + \frac{1}{\underline{g}_1}\mu_1 z_1(f_1 + g_1\varpi_2 + g_1\alpha_1 + d_1 - \dot{y}_r - \dot{\phi}e(0)) + \frac{1}{\underline{g}_1}\mu_2 z_1 - \frac{1}{h_1}\tilde{\theta}_1\dot{\hat{\theta}}_1 - \frac{1}{\upsilon_1}\tilde{\beta}_1\dot{\hat{\beta}}_1 + \varpi_2\dot{\varpi}_2$. By following the same line from (16) to (19), it can be derived that $\frac{1}{\underline{g}_1}z_1\dot{z}_1 \leqslant \mu_1^2 z_1^2 z_2^2 + \frac{g_1}{\underline{g}_1}\mu_1 z_1\alpha_1 + z_1\Xi_1 + \mu_1^2 z_1^2\Psi_1^2\tilde{\theta}_1 + \frac{2}{\pi}\mu_1 z_1\tilde{\beta}_1\arctan(\frac{\mu_1 z_1}{\sigma_1}) + \frac{1}{4}\varpi_2^4 + \Pi_1'$, where $\sigma_1 > 0$ is a design parameter; $\Xi_1 = \mu_1^2 z_1\Psi_1^2\hat{\theta}_1 + \frac{2}{\pi}\mu_1\hat{\beta}_1\arctan(\frac{\mu_1 z_1}{\sigma_1}) + \mu_1^2 z_1 + \mu_2^2 z_1 + \mu_1^2 z_1\dot{y}_r^2 + \mu_1^2 z_1\dot{\phi}^2 e^2(0)$; $\Pi_1' = \frac{2}{\pi}\beta_1\sigma_1 + \frac{\overline{g}_1^2}{4\underline{g}_1^2} + \frac{\overline{g}_1^4}{16\underline{g}_1^4} + \frac{1}{\underline{g}_1^2}$. Then, design the virtual control law, α_1, and the update laws for $\hat{\theta}_1$ and $\hat{\beta}_1$ as

$$\begin{cases} \alpha_1 = -\frac{1}{\mu_1}\left(k_1 z_1 + \Xi_1 + \gamma_l\Delta_l z_1 + \gamma_u\Delta_u z_1\right), \\ \dot{\hat{\theta}}_1 = h_1\mu_1^2 z_1^2\Psi_1^2 - l_1\hat{\theta}_1, \quad \hat{\theta}_1(0) \geqslant 0, \\ \dot{\hat{\beta}}_1 = \frac{2}{\pi}\upsilon_1\mu_1 z_1\arctan(\frac{\mu_1 z_1}{\sigma_1}) - m_1\hat{\beta}_1, \quad \hat{\beta}_1(0) \geqslant 0, \end{cases} \tag{40}$$

where k_1, γ_l, γ_u, l_1, and m_1 are positive design constants, and $-\gamma_l\Delta_l z_1/\mu_1$ and $-\gamma_u\Delta_u z_1/\mu_1$ are the differentiable terms. Inserting $\frac{1}{\underline{g}_1}z_1\dot{z}_1$ and (40) into $\dot{V}_1$ and utilizing $\frac{1}{4}\varpi_2^4 + \varpi_2\dot{\varpi}_2 \leqslant (\frac{1}{2} - \frac{1}{\varepsilon_2})\varpi_2^4 + \frac{1}{2}\Lambda_1^2 + \frac{1}{4}$ with $\Lambda_1 = \dot{\alpha}_1$ yield $\dot{V}_1 \leqslant \mu_1^2 z_1^2 z_2^2 - k_1 z_1^2 - \gamma_l\Delta_l z_1^2 - \gamma_u\Delta_u z_1^2 + \frac{l_1}{h_1}\tilde{\theta}_1\hat{\theta}_1 + \frac{m_1}{\upsilon_1}\tilde{\beta}_1\hat{\beta}_1 + (\frac{1}{2} - \frac{1}{\varepsilon_2})\varpi_2^4 + \frac{1}{2}\Lambda_1^2 + \Gamma_1' \leqslant \mu_1^2 z_1^2 z_2^2 - k_1 z_1^2 + \frac{l_1}{h_1}\tilde{\theta}_1\hat{\theta}_1 + \frac{m_1}{\upsilon_1}\tilde{\beta}_1\hat{\beta}_1 - c_2\varpi_2^4 + \frac{1}{2}\Lambda_1^2 + \Gamma_1'$, where $\Gamma_1' = \Pi_1' + \frac{1}{4}$ and $0 < \varepsilon_2 < 1/(\frac{1}{2} + c_2)$ with $c_2 > 0$ being a constant. It is notable that the introduction of $-\gamma_l\Delta_l z_1/\mu_1$ and $-\gamma_u\Delta_u z_1/\mu_1$ in (40) does not make the structure of $\dot{V}_1$ more complicated, as a result of $-\gamma_l\Delta_l z_1^2 \leqslant 0$ and $-\gamma_u\Delta_u z_1^2 \leqslant 0$ with $\Delta_l \geqslant 0$, $\Delta_u \geqslant 0$, and $z_1^2 \geqslant 0$.

Step i $(i = 2, \ldots, n-1)$**.** Following the same design procedure as in Section 3 to devise the virtual control laws, $\alpha_2, \ldots, \alpha_{n-1}$, and the update laws for $\hat{\theta}_2, \ldots, \hat{\theta}_{n-1}$ and $\hat{\beta}_2, \ldots, \hat{\beta}_{n-1}$ one by one, we can obtain

$$\begin{cases} \alpha_2 = -\left(k_2 z_2 + \mu_1^2 z_1^2 z_2 + \Phi_2\right), \\ \alpha_i = -\left(k_i z_i + z_{i-1}^2 z_i + \Phi_i\right), \quad i = 3, \ldots, n-1, \\ \dot{\hat{\theta}}_i = h_i z_i^2\Psi_i^2 - l_i\hat{\theta}_i, \quad \hat{\theta}_i(0) \geqslant 0, \quad i = 2, \ldots, n-1, \\ \dot{\hat{\beta}}_i = \frac{2}{\pi}\upsilon_i z_i\arctan(\frac{z_i}{\sigma_i}) - m_i\hat{\beta}_i, \quad \hat{\beta}_i(0) \geqslant 0, \quad i = 2, \ldots, n-1, \end{cases} \tag{41}$$

where k_i, h_i, l_i, υ_i, σ_i, and m_i are positive design parameters, $i = 2, \ldots, n-1$, and $\Phi_i = z_i\Psi_i^2\hat{\theta}_i + \frac{2}{\pi}\hat{\beta}_i\arctan(\frac{z_i}{\sigma_i}) + z_i + z_i\dot{\alpha}_{i,f}^2$, $i = 2, \ldots, n-1$. Construct the Lyapunov function candidate as $V_i = V_{i-1} + \frac{1}{2\underline{g}_i}z_i^2 + \frac{1}{2h_i}\tilde{\theta}_i^2 + \frac{1}{2\upsilon_i}\tilde{\beta}_i^2 + \frac{1}{2}\varpi_{i+1}^2$, $i = 2, \ldots, n-1$, where $\tilde{\theta}_i = \theta_i - \hat{\theta}_i$ and $\tilde{\beta}_i = \beta_i - \hat{\beta}_i$ with $\theta_i = \delta_i^2$ and $\beta_i = \frac{\overline{d}_i}{\underline{g}_i}$, $i = 2, \ldots, n-1$. Computing the time derivative of V_i and invoking $\dot{V}_1$ and (41), we obtain $\dot{V}_i \leqslant z_i^2 z_{i+1}^2 - \sum_{j=1}^{i} k_j z_j^2 + \sum_{j=1}^{i}\frac{l_j}{h_j}\tilde{\theta}_j\hat{\theta}_j + \sum_{j=1}^{i}\frac{m_j}{\upsilon_j}\tilde{\beta}_j\hat{\beta}_j - \sum_{j=1}^{i} c_{j+1}\varpi_{j+1}^4 + \sum_{j=1}^{i}\frac{1}{2}\Lambda_j^2 + \sum_{j=1}^{i}\Gamma_j'$, where $\Gamma_i' = \Pi_i + \frac{1}{4}$ with $\Pi_i = \frac{2}{\pi}\beta_i\sigma_i + \frac{\overline{g}_i^2}{4\underline{g}_i^2} + \frac{\overline{g}_i^4}{16\underline{g}_i^4} + \frac{1}{2\underline{g}_i^2}$, $i = 2, \ldots, n-1$.

Step n**.** In the end, the actual control law, u, and the update laws for $\hat{\theta}_n$ and $\hat{\beta}_n$ are designed by

$$\begin{cases} u = -\left(k_n z_n + z_{n-1}^2 z_n + \Phi_n\right), \\ \dot{\hat{\theta}}_n = h_n z_n^2\Psi_n^2 - l_n\hat{\theta}_n, \quad \hat{\theta}_n(0) \geqslant 0, \\ \dot{\hat{\beta}}_n = \frac{2}{\pi}\upsilon_n z_n\arctan(\frac{z_n}{\sigma_n}) - m_n\hat{\beta}_n, \quad \hat{\beta}_n(0) \geqslant 0, \end{cases} \tag{42}$$

where k_n, h_n, l_n, υ_n, σ_n, and m_n are positive design parameters, and $\Phi_n = z_n\Psi_n^2\hat{\theta}_n + \frac{2}{\pi}\hat{\beta}_n \arctan(\frac{z_n}{\sigma_n}) + z_n\dot{\alpha}_{n,f}^2$. Consider the Lyapunov function candidate as $V_n = V_{n-1} + \frac{1}{2\underline{g}_n}z_n^2 + \frac{1}{2h_n}\tilde{\theta}_n^2 + \frac{1}{2\upsilon_n}\tilde{\beta}_n^2$, where $\tilde{\theta}_n = \theta_n - \hat{\theta}_n$ and $\tilde{\beta}_n = \beta_n - \hat{\beta}_n$ with $\theta_n = \delta_n^2$ and $\beta_n = \frac{\overline{d}_n}{\underline{g}_n}$. In view of $\dot{V}_{n-1}$ and (42), the differential equation for V_n is obtained by $\dot{V}_n \leqslant -\sum_{j=1}^n k_j z_j^2 + \sum_{j=1}^n \frac{l_j}{h_j}\tilde{\theta}_j\hat{\theta}_j + \sum_{j=1}^n \frac{m_j}{\upsilon_j}\tilde{\beta}_j\hat{\beta}_j - \sum_{j=1}^{n-1} c_{j+1}\varpi_{j+1}^4 + \sum_{j=1}^{n-1}\frac{1}{2}\Lambda_j^2 + \sum_{j=1}^{n-1}\Gamma_j' + \Pi_n$, where $\Pi_n = \frac{2}{\pi}\beta_n\sigma_n + \frac{1}{2\underline{g}_n^2}$.

Another theoretical result of this paper is summarized as follows.

Theorem 2. The proposed control scheme in (4), (5), (11), (33)–(37), (39), (40)–(42) solves Problem 2, under Assumptions 1–4 and any known bounded initial condition.

Proof. It can be carried out in a similar procedure with the proof of Theorem 1; thus, the main proof is omitted due to the limited space. However, what needs to be proven additionally is the boundedness of $\Delta_l(t)$ and $\Delta_u(t)$. Similarly to (31), we can derive that V_n is bounded for all $t \geqslant 0$. This implies that z_i, $\hat{\theta}_i$, $\hat{\beta}_i$ and ϖ_j are uniformly bounded, $i = 1, \ldots, n$, $j = 2, \ldots, n$. According to the boundedness of θ_i and β_i, one sees from $\tilde{\theta}_i = \theta_i - \hat{\theta}_i$ and $\tilde{\beta}_i = \beta_i - \hat{\beta}_i$ that $\hat{\theta}_i$ and $\hat{\beta}_i$ are uniformly bounded, $i = 1, \ldots, n$. By (33) and Lemma 3, there hold $F_l(t) \in \mathcal{L}^\infty$ and $F_u(t) \in \mathcal{L}^\infty$. On this basis, we obtain $\xi(t) \in \mathcal{L}^\infty$ and $e(t) \in \mathcal{L}^\infty$. This together with Table 1 yields that there exists a positive constant, $\bar{\delta}_i$, such that $0 \leqslant \delta_i(t) < \bar{\delta}_i$ for all $t \geqslant 0$, $i \in \{l, u\}$. Then, invoking Lemma 2, we deduce that $\Delta_l(t)$ in (34) and $\Delta_u(t)$ in (35) are uniformly bounded under $\Delta_l(0) = 0$ and $\Delta_u(0) = 0$.

Remark 9. It follows from (32) that the self-adjustable prescribed performance is manifested in two aspects. On the one hand, under $\Delta_l(0) = 0$ and $\Delta_u(0) = 0$, we obtain from (33) that $\omega_l(0) = 0$ and $\omega_u(0) = 0$. This together with (4) yields by (32) for $t = 0$ that $-\rho_l(0) + e(0) < e(0) < \rho_u(0) + e(0)$. Accordingly, whenever the controlled system is rerun, or the reference is changed, our approach is capable of automatically adjusting the initial values of the upper and lower performance boundaries on $e(t)$, i.e., $(\rho_u(0) + e(0))$ and $(-\rho_l(0) + e(0))$, such that the initial condition holds naturally. On the other hand, in the presence of paroxysmal factors, e.g., a disturbance with a large amplitude of change, the performance boundaries on the tracking error are temporarily modified based on the user-appointed rules in (32)–(35) such that the performance specifications are appropriately relaxed and the tracking control task becomes more feasible. The design philosophy is clarified in Remark 8. Moreover, in (40), a pair of differentiable terms, $-\gamma_l\Delta_l z_1/\mu_1$ and $-\gamma_u\Delta_u z_1/\mu_1$, are employed to compensate for the negative effects arising from the violent variation of the tracking error, thus strengthening the robustness of the control system to prevent instability during operation. In addition to the relaxation of the performance specifications, this is another essential difference between the proposed approach in this section and that in Section 3. In this direction, the following example is provided to illustrate the roles of the modification signals, $\omega_l(t)$ and $\omega_u(t)$, in (32) and the auxiliary terms, $-\gamma_l\Delta_l z_1/\mu_1$ and $-\gamma_u\Delta_u z_1/\mu_1$, in (40) for control implementation.

Example 2. Consider the longitudinal vehicle system in Example 1 again. According to Theorem 2, a controller, labeled as C_1, is obtained with $T_f = 3$, $\lambda = 1$, $\rho_{l,0} = \rho_{u,0} = 0.2$, $\ell_l = \ell_u = 1$, $\tilde{T}_l = \tilde{T}_u = 3$, $\rho_{l,\tilde{T}} = \rho_{u,\tilde{T}} = 0.05$, $k_1 = 20$, $\gamma_l = \gamma_u = 50$, $\sigma_1 = 0.02$, $k_2 = 200$, $\sigma_2 = 0.02$, $\varepsilon_1 = 0.001$, $h_1 = h_2 = 5$, $l_1 = l_2 = 20$, $\upsilon_1 = \upsilon_2 = 1$, $m_1 = m_2 = 3$, $\Psi(\vartheta) = (\vartheta - 1)^2$, $p_{1,l} = p_{1,u} = 0.5$, $p_{2,l} = p_{2,u} = 110$, $p_{3,l} = p_{3,u} = 50$, and $p_{4,l} = p_{4,u} = 0.5$. To evaluate the impact of the auxiliary terms in (40) on the control performance, a comparative controller, labeled as C_2, is employed to conduct an ablation study, i.e., the above controller with $\gamma_l = \gamma_u = 0$. The simulation is performed under MATLAB with the 0.0 start time, the 10 stop time, the fixed-step type, and the 0.001 FST. Apply the above two controllers to the longitudinal vehicle system under the same initial conditions with Example 1, and the simulation results are displayed in Figure 5. It is seen that the tracking errors evolve inside their respective performance envelopes, despite the abrupt change in the amplitude of $d_1(t)$ shown in Figure 4(c), unlike the result in Figure 4(a). Nevertheless, careful inspection of Figure 5 reveals that the tracking error obtained by C_1 exhibits a lower amplitude during the abrupt change in the amplitude of the external disturbance than that under C_2. This is attributed to the compensation of the auxiliary terms in (40) for the negative effects caused by the disturbance. Therefore, the combination of the modification signals in (32) and the auxiliary terms in (40) is capable of effectively enhancing the reliability of control implementation under low-frequency sampling when a disturbance with a large amplitude of change is present. In this spirit, the proposed approach in this paper is also suitable for some practical scenarios in addition to Example 1, including the unmanned aerial vehicles flying under microburst [40], the waverider vehicles flying under sudden disturbances [45], the hypersonic vehicles with a drastically changing reference [46],

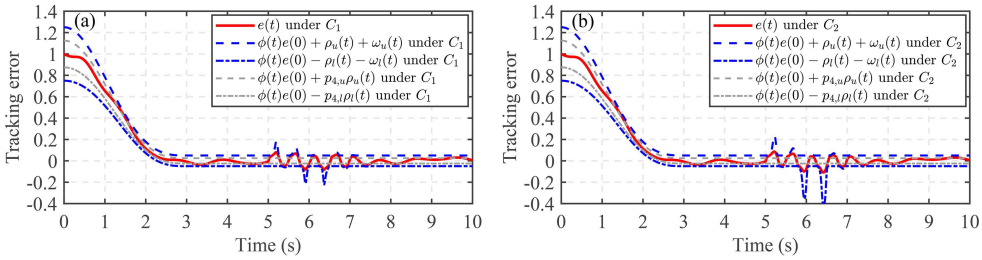

Figure 5 (Color online) Evolutions of the tracking errors. (a) $e(t)$ obtained by C_1; (b) $e(t)$ obtained by C_2.

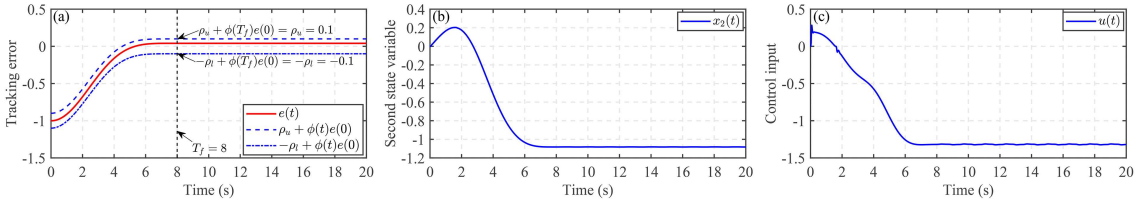

Figure 6 (Color online) Simulation under our approach. (a) The tracking error and performance envelope; (b) the second state variable; (c) the control input.

and the mechanical systems under denial-of-service attacks [47].

5 Simulation studies

In this section, three simulation studies are conducted to illustrate the above theoretical results.

Example 3. Consider a second-order nonlinear system with the following dynamics:

$$\dot{x}_1 = x_1^2 + x_2, \quad \dot{x}_2 = x_1^3 x_2^2 + u, \quad y = x_1 \tag{43}$$

with $x_1(0) = 0$ and $x_2(0) = 0$. The control task for (43) is to drive $y(t)$ to track $y_r(t) = 1$, and the transient and steady-state tracking response is formulated by

$$|y(t) - y_r(t)| < 0.1, \quad t \geqslant 8. \tag{44}$$

Based on Theorem 1, a controller is formed with $\rho_l = \rho_u = 0.1$, $\lambda = 3$, $T_f = 8$, $k_1 = 35$, $\Psi_1(\overline{x}_1) = x_1^2$, $k_2 = 100$, $\Psi_2(\overline{x}_2) = x_1^2 x_2^2 e^{x_1}$, $\varepsilon_2 = 10^{-6}$, $h = 1$, and $l = 20$. The application of the above controller to (43) is depicted in Figure 6. It is seen that the tracking error evolves inside the performance envelope such that the performance requirement predefined in (44) is satisfied. Moreover, the second state variable and the control input are both bounded. Therefore, the feasibility of the developed approach is verified by the simulation results.

For comparison, another PPC scheme with a standard second-order transient response [34] is applied to (43) under the known system model. The simulation results are collected in Figure 7. It is observed from Figure 7(a) that since $\psi(t)$ is not identically equal to zero for $t \geqslant 8$, the actual performance constraint on the tracking error is $(-0.1 + \psi(t)e(0), 0.1 + \psi(t)e(0))$ rather than $(-0.1, 0.1)$ during $t \in [8, 20)$. This means that the performance requirement for the tracking accuracy is not fulfilled after the predefined settling time. On the other hand, the comparison between Figures 6 and 7 shows that a larger negative control peak is needed for the comparative scheme. Accordingly, the simulation results demonstrate the superiority of our approach.

Example 4. Consider the mathematical model of a jet engine compressor as follows [6]:

$$\dot{x}_1 = -x_2 - 1.5x_1^2 - 0.5x_1^3, \quad \dot{x}_2 = u + d(t), \quad y = x_1, \tag{45}$$

where x_1, x_2, u, and $d(t)$ denote the mass flow, the pressure rise, the throttle mass flow, and the disturbance, respectively. In the simulation, let $\overline{x}_2(0) = [1, 0]^{\mathrm{T}}$ and $d(t) = \sin(2t)$. The control objective for (45) is to steer $y(t)$ to track $y_r(t) = \sin(t)$ with the following performance specification:

$$|y(t) - y_r(t)| < 0.05, \quad t \geqslant 6. \tag{46}$$

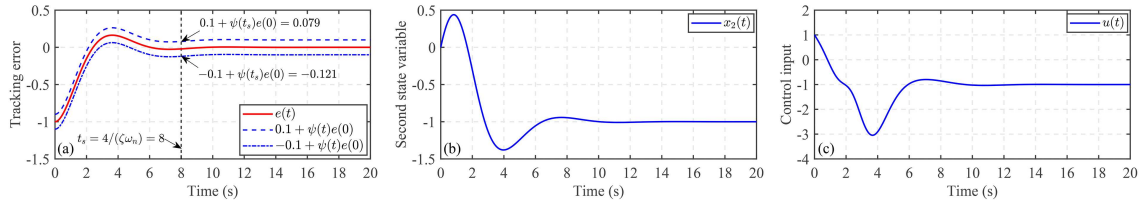

Figure 7 (Color online) Simulation under the comparative scheme [34]. (a) The tracking error and performance envelope; (b) the second state variable; (c) the control input.

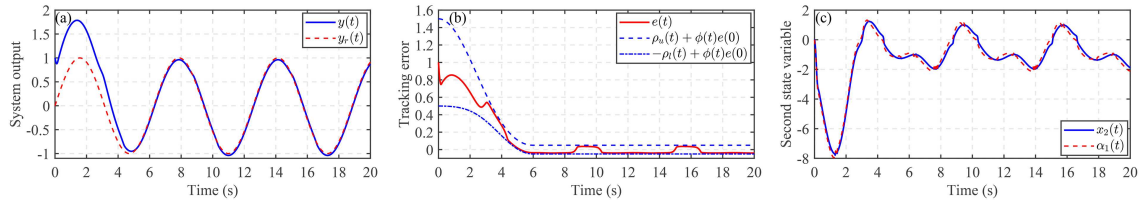

Figure 8 (Color online) Simulation under proposed control. (a) The system output and reference; (b) the tracking error and performance envelope; (c) the second state variable and virtual control signal.

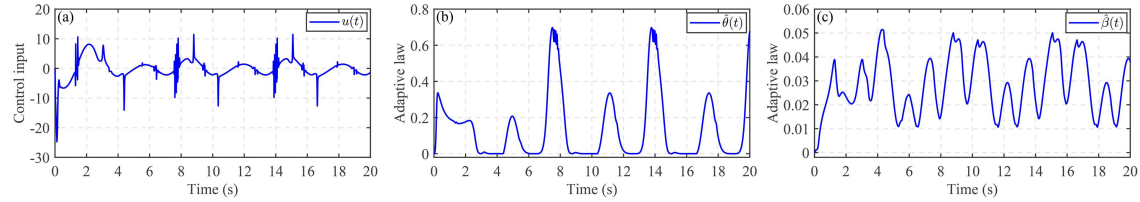

Figure 9 (Color online) Simulation under proposed control. (a) The control input; (b) the adaptive law $\hat{\theta}(t)$; (c) the adaptive law $\hat{\beta}(t)$.

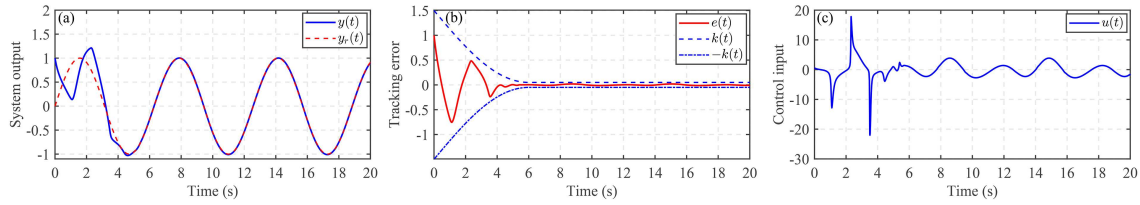

Figure 10 (Color online) Simulation under PI FC [11]. (a) The system output and reference; (b) the tracking error and performance envelope; (c) the control input.

Following Theorem 2, a controller is acquired with $T_f = 6$, $\lambda = 0.1$, $\rho_{l,0} = \rho_{u,0} = 0.45$, $\ell_l = \ell_u = 0.1$, $\tilde{T}_l = \tilde{T}_u = 6$, $\rho_{l,\tilde{T}} = \rho_{u,\tilde{T}} = 0.05$, $k_1 = 2$, $\gamma_l = \gamma_u = 0$, $k_2 = 5$, $\sigma_2 = 0.02$, $\varepsilon_1 = 0.0001$, $h = 1$, $l = 20$, $\upsilon = 1$, $m = 3$, $\Psi_1(x_1) = x_1^2(e^{x_1} + 2)$, $p_{i,l} = p_{i,l} = 0$, $i = 1, 2, 3$, and $p_{4,l} = p_{4,u} = 0.99$. Apply it to (45), and the simulation results are displayed in Figures 8 and 9. It is observed from Figure 8(a) that reference tracking is achieved. Concretely, Figure 8(b) exhibits the evolution of the tracking error inside the performance envelope, thus fulfilling the performance requirement in (46). One sees from Figures 8(c) and 9 that the second state variable, the virtual control signal, the control input, and the adaptive laws are all bounded. Thus, the feasibility of the proposed approach is verified by the simulation results.

For the purpose of comparison, a proportional-integral (PI) FC scheme [11] is applied to (45) with the same control objective. Figure 10 displays the simulation results. It is seen that reference tracking is realized by a bounded control input, and the tracking error fulfills the performance requirement in (46). Nevertheless, careful inspection of Figures 8(b) and 10(b) reveals that the tracking error obtained by our controller exhibits a smaller overshoot than that by using the PI funnel controller. This is because our approach is capable of regulating quantitatively the error overshoot by imposing a tight performance envelope on the tracking error. Accordingly, the comparative simulation results clarify the advantage of the proposed control approach.

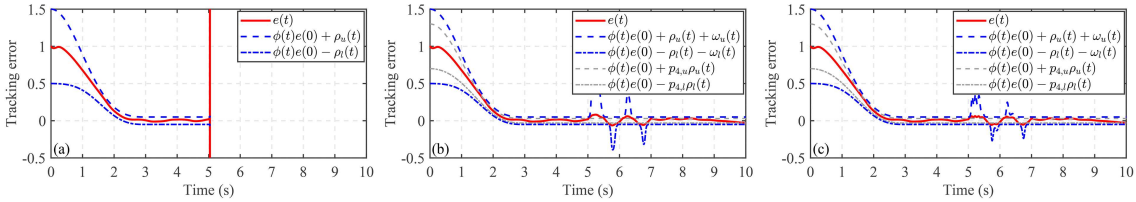

Figure 11 (Color online) Simulation under different cases. (a) The tracking error and performance envelope under Case 1; (b) the tracking error and performance envelope under Case 2; (c) the tracking error and performance envelope under Case 3.

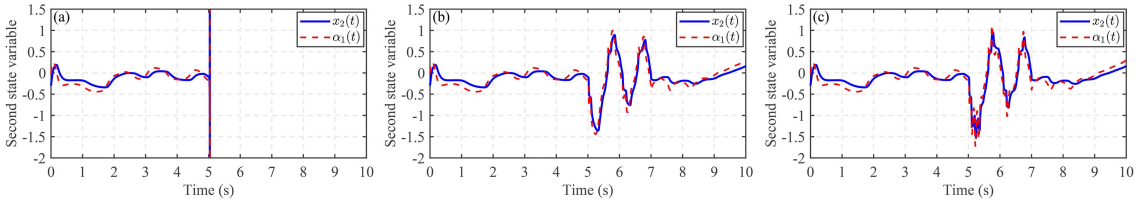

Figure 12 (Color online) Simulation under different cases. (a) The second state variable and virtual control signal under Case 1; (b) the second state variable and virtual control signal under Case 2; (c) the second state variable and virtual control signal under Case 3.

Example 5. To further enrich the simulation test, consider the following strict-feedback system:

$$\begin{cases} \dot{x}_1 = 0.5\sin(0.1x_1) + (1.5 + 0.2\sin(0.3x_1))x_2 + d_1(t), \\ \dot{x}_2 = 0.1\sin(x_1x_2) + 0.2\mathrm{e}^{-|x_1|+1} + (1.5 + 0.2\cos(0.1x_1x_2))u + d_2(t), \\ y = x_1, \end{cases} \tag{47}$$

where $x_1(0) = 1$ and $x_2(0) = -0.3$; $d_1(t) = 0.1\sin(5t)$ for $0 \leqslant t < 5$, $d_1(t) = 1.25\sin(2\pi t) - 0.5\cos(3(t-2))$ for $5 \leqslant t < 7$, and $d_1(t) = 0.2\cos(1.5t)$ for $t \geqslant 7$, which simulates a disturbance with a large amplitude of change; $d_2(t) = 1.2\sin(t) + 0.75\cos(t)$. The control task is to force $y(t)$ to track $y_r(t) = 0.5\sin(0.5t)$ with the anticipant performance guarantees:

$$\phi(t)e(0) - \rho_l(t) - \omega_l(t) < y(t) - y_r(t) < \phi(t)e(0) + \rho_u(t) + \omega_u(t), \quad t \geqslant 0. \tag{48}$$

According to Theorem 2, the design parameters of the control approach are chosen as $\lambda = 1$, $T_f = 3$, $\rho_{l,0} = \rho_{u,0} = 0.45$, $\rho_{l,\tilde{T}} = \rho_{u,\tilde{T}} = 0.05$, $\ell_l = \ell_u = 1$, $\tilde{T}_l = \tilde{T}_u = 3$, $p_{2,l} = p_{2,u} = 50$, $p_{1,l} = p_{1,u} = 0.5$, $p_{4,l} = p_{4,u} = 0.6$, $k_1 = 10$, $\sigma_1 = 0.02$, $k_2 = 12$, $\sigma_2 = 0.02$, $\varepsilon_2 = 0.001$, $h_1 = h_2 = 5$, $l_1 = l_2 = 20$, $\upsilon_1 = \upsilon_2 = 1$, and $m_1 = m_2 = 3$. In our approach, the purpose of introducing $\omega_i(t)$ and $-\gamma_i\Delta_i(t)z_1(t)/\mu_1(t)$ is to enhance the reliability of control implementation in the case of low-frequency sampling, $i \in \{l, u\}$. For a sufficient demonstration of such a feature, three scenarios are considered as follows.

- **Case 1.** $\omega_i(t) = 0$ ($p_{3,i} = 0$) and $-\gamma_i\Delta_i(t)z_1(t)/\mu_1(t) = 0$ ($\gamma_i = 0$), $i \in \{l, u\}$.
- **Case 2.** $\omega_i(t) \geqslant 0$ ($p_{3,i} = 110$) and $-\gamma_i\Delta_i(t)z_1(t)/\mu_1(t) = 0$ ($\gamma_i = 0$), $i \in \{l, u\}$.
- **Case 3.** $\omega_i(t) \geqslant 0$ ($p_{3,i} = 110$) and $-\gamma_i\Delta_i(t)z_1(t)/\mu_1(t) \in \mathbb{R}$ ($\gamma_i = 6$), $i \in \{l, u\}$.

The simulation is performed under MATLAB with the 0.0 start time, the 10 stop time, the fixed-step type, and the 0.001 FST. The comparative simulation results are exhibited in Figures 11–14. The trajectories of the tracking errors under Cases 1–3 and their respective performance envelopes are plotted in Figure 11, from which we observe that the abrupt change of the disturbance causes a violation of the performance constraint in Case 1. By contrast, the constraint satisfaction of Cases 2 and 3 is achieved due to the introduction of $\omega_i(t)$ related to $\Delta_i(t)$ in (48), $i \in \{l, u\}$, where it is seen from Figure 14 that $\Delta_i(t)$, $i \in \{l, u\}$, is bounded and nonnegative. In addition, Figure 11 shows that the tracking performance of Case 3 is better than that of Case 2, since $-\gamma_i\Delta_i(t)z_1(t)/\mu_1(t)$, $i \in \{l, u\}$, introduced in the virtual control signal, compensates well for the effect of the disturbance on the tracking performance at the expense of more obvious fluctuations of the control signal, as depicted in Figure 13. Accordingly, the feasibility of our approach is verified by the simulation results.

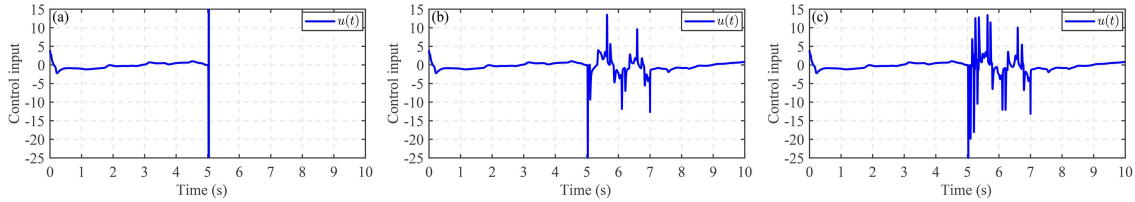

Figure 13 (Color online) Simulation under different cases. (a) The control input under Case 1; (b) the control input under Case 2; (c) the control input under Case 3.

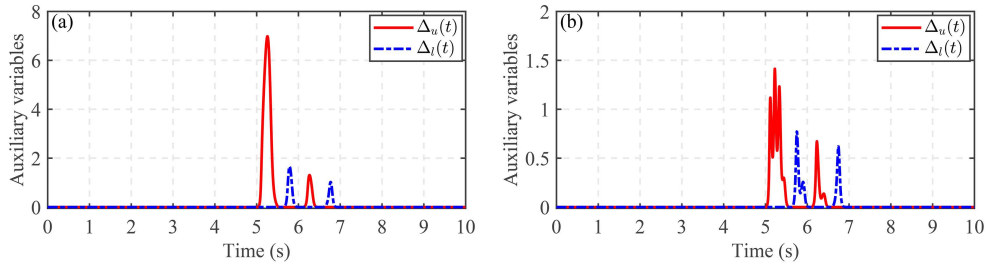

Figure 14 (Color online) Simulation under different cases. (a) The auxiliary variables under Case 2; (b) the auxiliary variables under Case 3.

6 Conclusion

An adaptive robust control approach with tight performance guarantees for the strict-feedback systems with parametric uncertainties and unmatched disturbances is put forward in this paper. It achieves reference tracking with the predefined performance specifications on the overshoot, the settling time, and the accuracy while guaranteeing the natural satisfaction of the initial condition. Moreover, the reliability of control implementation is enhanced by employing a kind of performance function with a self-adjustable ability and a pair of auxiliary terms for adaption of the control gain, in the presence of paroxysmal factors, e.g., a disturbance with a large amplitude of change. The simulation results validate the feasibility and advantages of the proposed approach. As future work, it is of interest to extend the established results to more complicated systems, e.g., nonlinear multiagent systems or multiple-input-multiple-output nonlinear systems.

Acknowledgements This work was supported in part by National Natural Science Foundation of China (Grant No. 62473089), Research Program of the Liaoning Liaohe Laboratory (Grant No. LLL23ZZ-05-01), 111 Project 2.0 of China (Grant No. B08015), National Key Research and Development Program of China (Grant No. 2022YFB3305905), Xingliao Talent Program of Liaoning Province of China (Grant No. XLYC2203130), Natural Science Foundation of Liaoning Province of China (Grant No. 2024JH3/10200012), Open Research Project of the State Key Laboratory of Industrial Control Technology of China (Grant No. ICT2024B12), and Fundamental Research Funds for the Central Universities of China (Grant Nos. N2424016, N25YJS002).

References

1 Swaroop D, Hedrick J K, Yip P P, et al. Dynamic surface control for a class of nonlinear systems. IEEE Trans Automat Contr, 2000, 45: 1893–1899
2 Wang D, Huang J. Neural network-based adaptive dynamic surface control for a class of uncertain nonlinear systems in strict-feedback form. IEEE Trans Neural Netw, 2005, 16: 195–202
3 Yu J P, Shi P, Chen X K, et al. Finite-time command filtered adaptive control for nonlinear systems via immersion and invariance. Sci China Inf Sci, 2021, 64: 192202
4 Xing L, Wen C, Liu Z, et al. Event-triggered adaptive control for a class of uncertain nonlinear systems. IEEE Trans Automat Contr, 2017, 62: 2071–2076
5 Liu Y, Li H, Lu R, et al. An overview of finite/fixed-time control and its application in engineering systems. IEEE CAA J Autom Sin, 2022, 9: 2106–2120
6 Krstić M, Kokotović P V. Lean backstepping design for a jet engine compressor model. In: Proceedings of IEEE Conference on Control Technology and Applications (CCTA), New York, 1995. 1047–1052
7 Kaufman H, Barkana I, Sobel K. Direct Adaptive Control Algorithms: Theory and Applications. New York: Springer, 1998
8 Ilchmann A, Ryan E P, Sangwin C J. Tracking with prescribed transient behaviour. ESAIM-Control Optim Calc Var, 2002, 7: 471–493
9 Ilchmann A, Ryan E P, Townsend P. Tracking with prescribed transient behavior for nonlinear systems of known relative degree. SIAM J Control Optim, 2007, 46: 210–230
10 Berger T, Lê H H, Reis T. Funnel control for nonlinear systems with known strict relative degree. Automatica, 2018, 87: 345–357
11 Zhang J X, Chai T. Proportional-integral funnel control of unknown lower-triangular nonlinear systems. IEEE Trans Automat Contr, 2024, 69: 1921–1927
12 Zhang J X, Ding J, Chai T. Cyclic performance monitoring-based fault-tolerant funnel control of unknown nonlinear systems with actuator failures. IEEE Trans Automat Contr, 2025. doi: 10.1109/TAC.2025.3550352

13 Bechlioulis C P, Rovithakis G A. Robust adaptive control of feedback linearizable MIMO nonlinear systems with prescribed performance. IEEE Trans Automat Contr, 2008, 53: 2090–2099
14 Zhang J X, Yang G H. Low-complexity tracking control of strict-feedback systems with unknown control directions. IEEE Trans Automat Contr, 2019, 64: 5175–5182
15 Fotiadis F, Rovithakis G A. Prescribed performance control for discontinuous output reference tracking. IEEE Trans Automat Contr, 2021, 66: 4409–4416
16 Shi Y, Yi B, Xie W, et al. Enhancing prescribed performance of tracking control using monotone tube boundaries. Automatica, 2024, 159: 111304
17 Zhang J X, Cui E Y, Shi P. Low-complexity high-performance control of unknown block-triangular MIMO nonlinear systems. IEEE Trans Ind Electron, 2025, 72: 7515–7523
18 Shi W, Hou M, Duan G, et al. Adaptive dynamic surface asymptotic tracking control of uncertain strict-feedback systems with guaranteed transient performance and accurate parameter estimation. Intl J Robust Nonlinear, 2022, 32: 6829–6848
19 Sui S, Chen C L P, Tong S. A novel full errors fixed-time control for constraint nonlinear systems. IEEE Trans Automat Contr, 2023, 68: 2568–2575
20 Liu X, Wang H, Gao C, et al. Adaptive fuzzy funnel control for a class of strict feedback nonlinear systems. Neurocomputing, 2017, 241: 71–80
21 Liu Y, Liu X, Jing Y, et al. A novel finite-time adaptive fuzzy tracking control scheme for nonstrict feedback systems. IEEE Trans Fuzzy Syst, 2019, 27: 646–658
22 Song Y D, Zhou S. Tracking control of uncertain nonlinear systems with deferred asymmetric time-varying full state constraints. Automatica, 2018, 98: 314–322
23 Zhang J X, Wang Q G, Ding W. Global output-feedback prescribed performance control of nonlinear systems with unknown virtual control coefficients. IEEE Trans Automat Contr, 2022, 67: 6904–6911
24 Li F Z, Liu Y G. Global practical tracking with prescribed transient performance for inherently nonlinear systems with extremely severe uncertainties. Sci China Inf Sci, 2019, 62: 022204
25 Liu Y H, Su C Y, Li H. Adaptive output feedback funnel control of uncertain nonlinear systems with arbitrary relative degree. IEEE Trans Automat Contr, 2021, 66: 2854–2860
26 Zhao K, Song Y, Chen C L P, et al. Adaptive asymptotic tracking with global performance for nonlinear systems with unknown control directions. IEEE Trans Automat Contr, 2022, 67: 1566–1573
27 Zhang J X, Chai T. Global prescribed performance control of unknown strict-feedback systems with quantized references. IEEE Trans Syst Man Cybern Syst, 2023, 53: 6257–6267
28 Cao Y, Cao J, Song Y. Practical prescribed time tracking control over infinite time interval involving mismatched uncertainties and non-vanishing disturbances. Automatica, 2022, 136: 110050
29 Wang Y, Liu Y G. Global adaptive output-feedback tracking with prescribed performance for uncertain nonlinear systems. Sci China Inf Sci, 2024, 67: 152201
30 Zhao K, Lewis F L, Zhao L. Unifying performance specifications in tracking control of MIMO nonlinear systems with actuation faults. Automatica, 2023, 155: 111102
31 Xie H, Zhang J X, Jing Y, et al. Self-adjustable performance-based adaptive tracking control of uncertain nonlinear systems. IEEE Trans Automat Sci Eng, 2025, 22: 750–764
32 Li L, Zhao K, Zhang Z, et al. Dual-channel event-triggered robust adaptive control of strict-feedback system with flexible prescribed performance. IEEE Trans Automat Contr, 2024, 69: 1752–1759
33 Liu Y H, Li H. Adaptive asymptotic tracking using barrier functions. Automatica, 2018, 98: 239–246
34 Wang Z, Liu X, Wang W. Prescribed performance control with a standard second-order transient response for strict feedback affine nonlinear systems. Int J Syst Sci, 2021, 52: 2677–2688
35 Wang Z, Liu X, Wang W. Adaptive prescribed performance control with selected transient response for a class of nonlinear systems with uncertainties. Int J Adapt Control Signal Process, 2022, 36: 670–689
36 Shen L, Wang H, Yue H. Prescribed performance adaptive fuzzy control for affine nonlinear systems with state constraints. IEEE Trans Fuzzy Syst, 2022, 30: 5351–5360
37 Habibi H, Yazdani A, Darouach M, et al. Observer-based sensor fault-tolerant control with prescribed tracking performance for a class of nonlinear systems. IEEE Trans Automat Contr, 2023, 68: 8259–8266
38 Xie H, Jing Y, Zhang J X, et al. Low-complexity tracking control of unknown strict-feedback systems with quantitative performance guarantees. IEEE Trans Cybern, 2024, 54: 5887–5900
39 Ji R, Ge S S, Zhao K. Coded event-triggered control for nonlinear systems. Automatica, 2024, 167: 111753
40 Yong K, Chen M, Shi Y, et al. Flexible performance-based control for nonlinear systems under strong external disturbances. IEEE Trans Cybern, 2024, 54: 762–775
41 Yong K, Chen M, Shi Y, et al. Flexible performance-based robust control for a class of nonlinear systems with input saturation. Automatica, 2020, 122: 109268
42 Ji R, Ge S S, Li D. Saturation-tolerant prescribed control for nonlinear systems with unknown control directions and external disturbances. IEEE Trans Cybern, 2024, 54: 877–889
43 Fotiadis F, Rovithakis G A. Input-constrained prescribed performance control for high-order MIMO uncertain nonlinear systems via reference modification. IEEE Trans Automat Contr, 2024, 69: 3301–3308
44 Berger T. Input-constrained funnel control of nonlinear systems. IEEE Trans Automat Contr, 2024, 69: 5368–5382
45 Bu X, Lv M, Lei H, et al. Fuzzy neural pseudo control with prescribed performance for waverider vehicles: a fragility-avoidance approach. IEEE Trans Cybern, 2023, 53: 4986–4999
46 Wang Y, Hu J, Li J, et al. Improved prescribed performance control for nonaffine pure-feedback systems with input saturation. Intl J Robust Nonlinear, 2019, 29: 1769–1788
47 Yong K, Chen M, Liu W, et al. Flexible performance-based neural network control for mechanical systems under DoS attack and event triggering. IEEE ASME Trans Mechatron, 2023, 28: 2119–2130
48 Krstić M, Kanellakopoulos I, Kokotović P V. Nonlinear and Adaptive Control Design. New York: Wiley, 1995
49 Jin X, Dai S L, Liang J. Adaptive constrained formation-tracking control for a tractor-trailer mobile robot team with multiple constraints. IEEE Trans Automat Contr, 2023, 68: 1700–1707